Physics – Uspekhi **43** (4) 381 – 406 (2000)

REVIEWS OF TOPICAL PROBLEMS

PACS numbers: **89.60.+x**, **92.60.–e**, 92.60.Ry, **92.90.+x**

Climate as a problem of physics

A S Monin, Yu A Shishkov

DOI: 10.1070/PU2000v043n04ABEH000678

Contents

Abstract. The logical fundamentals of the theory of climate are outlined: (1) the climate system OLA (ocean – land – atmosphere) is defined; (2) analogously to the theory of turbulence, the notion of climate is defined as a multicomponent random function in the OLA space-time (or, equivalently, as a statistical ensemble of states the OLA system passes through in a period of several decades); (3) the solar climate, i.e. the distribution of solar radiation at the upper atmosphere boundary, is determined, to be employed as the boundary condition for the OLA system; (4) the 'horizontal' heat and mass transfer processes between the equatorial and polar zones are described; (5) the 'vertical' processes of radiative – convective heat and mass transfer, among them the greenhouse effect of water vapor and small gas admixtures, are discussed; (6) the 'vertical' radiative heat transfer processes in an aerosol-containing atmosphere is considered, including the anti-greenhouse effect of volcanic and smoke aerosols, and the 'nuclear night' and 'nuclear winter' scenarios.

1. Introduction

Climatic changes are perceivable by the human community. The 'memory of generations' keeps track of such changes, they are passed down in oral tradition, recorded in chronicles, and in recent centuries they have been registered using instrumental methods (the longest series of measurements of ambient temperature, covering 335 years, has been compiled for Central England by Gordon Manley [1, 2]).

In this way, we have learned about the 'Little Ice Age' (LIA) that started with an abrupt and deep chill with a double minimum in 1570 and 1600, and ended with three deep cold waves in the 19th century. Since 1866 there has been a general retreat of glaciers in the Alps (see in Fig. 1 the summary trend of summer temperatures in the northern hemisphere over the period of 1400 to 1970 compiled by Bradley and Jones [3], who supplemented the measurement data with circumstantial evidence like the annual rings of trees, information on melting of glaciers, and written records).

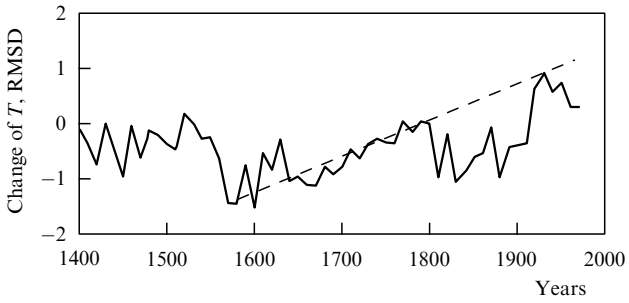

Figure 1. Oscillations of summer temperatures in the northern hemisphere during the Little Ice Age, according to Bradley and Jones [3]. The change is measured in units of long-term rms deviation (RMSD). Dashed line indicates the linear trend drawn through extremes.

The history of the LIA is discussed, for example, in Section 10.3 of the book [4]. It is pertinent to note that in 1300 – 1350 Iceland and Norway stopped growing cereals, and England abandoned its vineyards (switching to wines from France and port, and later starting the production of grain whiskey and juniper gin). The beginning of the LIA is recorded in the chronicles of Muscovy as a very early and strong frost that destroyed the crops — 'beaten by the great frost' — and caused devastating famine (mentioned by A S Pushkin in his poem 'Boris Godunov'). According to Koretsky, this happened on the 28th of July, and according to the New Chronicler on August 15, 1601 (see Ref. [5]).

We do not know what caused the LIA, nor why it came to an end. Presumably, this was due to natural causes, since the anthropogenic impact on the environment at that time should obviously have been small.

Abundant and diversified sources (some of which will be quoted later on) indicate that abrupt changes with a period of

A S Monin, Yu A Shishkov P P Shirshov Institute for Oceanology, Russian Academy of Sciences
ul. Krasikova 23, 117218 Moscow, Russian Federation
Tel. (7-095) 129 08 18. Fax (7-095) 124 59 83

Received 11 October 1999, revised 31 January 2000
Uspekhi Fizicheskikh Nauk **170** (4) 419–445 (2000)
Translated by A S Dobroslavskiĭ, edited by A Radzig

$10^0 - 10^5$ years are generally typical of the climate. The short-period spectrum (with the periods of $10^0 - 10^2$ years) may be referred to as the intermittency of the climate. Changes (anomalies) in the weather with periods ranging from several months to a few years would be more appropriately called long-term weather variations. They may be regional or global; in the latter case they may be called *climate vibrations* [6].

An example of such vibrations is given in Fig. 2, which shows the oscillation of mean annual temperatures for the Earth and for its northern and southern hemispheres over the last century, according to Hansen and Lebedeff [7, 8] (see also Hansen et al. [9]). We see that the temperature differences between succeeding years varied within $\pm 0.40\,^\circ$C (the mean absolute value was $0.12\,^\circ$C and increased at the transient periods — that is, the change of climate was not monotonic, but rather appeared as a background for the increasing vibrations of the climate system).

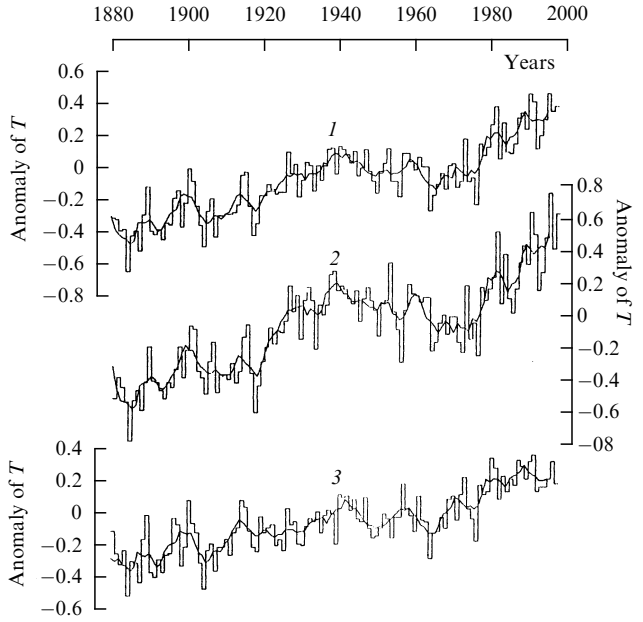

Figure 2. Vibrations of the average annual temperature on the globe (*1*), and in the northern (*2*) and southern (*3*) hemispheres over the course of the past century, according to Hansen and Lebedeff [7, 8]. Smooth curves were obtained by moving smoothing over a five-year period.

In this way, one of the most prominent features of the climate is its variability, and the main task of the theory of climate is the prediction of its change in the foreseeable future.

The majority of people are disturbed by news about climate change. One of the reasons is the ever-improving global information that increases public awareness of adverse weather anomalies which from time to time afflict different regions of the world and often result in disasters. These include: the droughts of 1968 – 1972 in the Sahel (a 5.2 million square kilometer semidesert strip south of Africa's Sahara Desert with a population of 60 million), which brought terrible famine; the drought and forest fires of 1972 in Eastern Europe; the drought of 1976 in Western Europe (''England without rain is like a ballerina without legs''); the droughts of 1977 and 1980 and the severe winters of 1978/79 and 1980/81 in North America, which depleted the world's stock of grain; the recent droughts and famine in Ethiopia and Somalia, etc.

Now are all these just transient local phenomena typical of the current climate, or indications of the deterioration of the global climate? And if the latter, is this deterioration a natural process or the direct result of anthropogenic impact — destruction of forests (whose area has by now decreased by 37%, while rain forests are now being destroyed at an annual rate of 114 thousand square kilometers), desertification (at an annual rate of 60 thousand square kilometers, or 20 hectares per minute), deterioration of soil (which has already led to the loss of 2 billion hectares of fertile land, compared with today's 1.5 billion hectares of arable land and pastures), emissions of carbon dioxide into the atmosphere as the result of fuel combustion (6 billion metric tons in terms of carbon per annum in recent years, or about one percent of its current content in the atmosphere), the increasing emission of industrial aerosols (with current annual production of 300 million tons) and freons, which rise into the stratosphere and destroy the Earth's ozone layer (the annual production of freons is currently estimated at 200 to 400 thousand tons), and so forth?

We do not yet have any trustworthy answers to these questions. What is more, we do not know which climate changes are good for us, and which are bad.

In common parlance, cooling is associated with the deterioration of climate, and warming with its improvement. As a matter of fact, however, apart from the temperature one must at least take humidity into account; then speculation about the 'quality' of climate becomes more complicated and starts to depend on the latitude and even on the particular region.

For example, using the series of average monthly temperatures for Central England according to Manley [1, 2] and the 226-year-long series of monthly precipitation totals according to Jones et al. [10], we find that, on average, the seasonal variation of precipitation has a minimum in April and a maximum in October, and that the temperatures and precipitation do not correlate on an annual basis, but show negative correlation in the warm half-year, and positive correlation in the cold half-year.

A similar tendency is observed in the LIA trends (Fig. 3) — that is, warming is accompanied by increased precipitation in the cold half-years and decreased precipitation in the warm half-years. It is quite possible, however, that this observation only applies to the LIA and the temperate zone. Numerical simulation has to give an indication of the temperature level at which this tendency can be overridden by the general increase in the moisture capacity of the entire atmosphere.

'Vibrations' shown in Fig. 2 as well as 'intermittency' of the climate, an example of which is given in Fig. 1, and to some extent the variations of climate over longer periods, give the impression of being chaotic and bring to mind the behavior of the dynamic systems which (in the modern theory of chaos) evolve on complex-structured limit sets present in their phase spaces and have come to be known as *strange attractors*. This concept was introduced by Edward Lorenz [11 – 13] [1].

In light of the above, the theory of climate variation ought to be the *statistical dynamics of the climate system*. Obviously, the construction of such a theory cannot be entrusted to geography — the science that had incorporated climatology up to the 1960s — and ought to be given over to physics. This

[1] The class of 'strange attractors' was discovered by the American mathematician Stephen Smale in the 1960s. (*Translator's note*.)

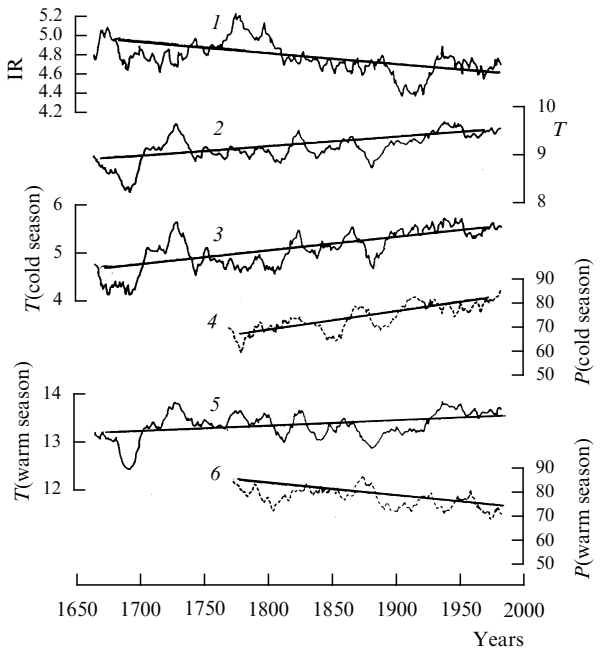

Figure 3. Trends of the Little Ice Age according to data subjected to moving averaging over a fifteen-year period: *1* — mean square ranges of seasonal temperature variation ('continentality indices'); *2* — mean annual temperatures; *3* and *5* — mean temperatures of cold and warm half-years; 4 and 6 — average monthly precipitation of cold and warm half-years.

is especially true because the study of climate in the past and present increasingly depends on physical approaches (first of all, isotopic methods).

Climate can be defined as a statistical ensemble of states passed by the climate system ocean–land–atmosphere (OLA) over a time period of several decades (see Section 2 for more details). The source of energy for the processes that take place in the climate system is solar radiation flux incident on the Earth. Its distribution over the upper atmosphere boundary in different seasons (known as the 'solar climate') is described in Section 3. An important feature is its latitudinal zoning. Owing to the smoothing effect of horizontal heat exchange due to atmospheric and oceanic circulation, however, the zoning of the conventional climate is not as sharp as that of the solar climate. The effect of horizontal heat exchange is described by the similarity theory presented in Section 4. Vertical heat exchange (radiative and convective) is responsible for the stratification of the atmosphere and is considered in Section 5. It involves absorption of solar radiation by the atmosphere and the underlying surface; part of the absorbed radiation is reradiated and absorbed by certain atmospheric components (natural and man-made) which create the 'greenhouse effect'. Finally, in Section 6 we discuss the 'anthropogenic effect' caused by atmospheric aerosols of natural (mainly volcanic) and anthropogenic origin (including the effects of very large explosions resulting from the possible impact of asteroids, or because of nuclear warfare — the so-called 'nuclear winter'). Similar factors shape the climates of other Earth-like planets. In the case of large planets, heating by solar radiation is supplemented by internal heating due to the continued compression of these planets.

Such an approach to the definition of climate was proposed in our books [4, 14, 15] (see also the corresponding definition of the climate of the ocean in Ref. [16]). It provided the basis for the international Global Atmospheric Research Program (GARP) launched in 1967 by the International Council of Scientific Unions (ICSU) and World Meteorological Organization (WMO) with the purpose of developing numerical models of general atmospheric circulation for long-term weather forecasts, and staging observational experiments for the collection of global initial data for such forecasts. This program was published in 1975 as a monograph [17] (some results of numerical simulations can be found in the brochure [18]).

Unfortunately, the execution of GARP was slow, and the first global experiment within the framework of this program took 13 years to start, and the coverage of oceans and the southern hemisphere was very fragmentary. The member countries decided not to launch another experiment, and the World Climate Program (WCP) was organized instead by the ICSU, WMO, and the Intergovernmental Oceanographic Commission of UNESCO. This program continues to operate to this day.

Its importance was emphasized in 1992 by the decisions of the UN Conference on environment and development in Rio de Janeiro [19], including the UN Convention on climate change, which sets restrictions on carbon dioxide dispersions to the atmosphere — although they are somewhat hasty and not sufficiently justified. On the other hand, however, any ecological restrictions are in principle always welcome. In general, the UN decisions lobbied by US corporations that resist ecological restrictions do not go far enough. In particular, this applies to the obscure concept of 'sustainable development' proclaimed in the decisions of the United Nations.

2. Definition of climate and climate system

The term climate (from Greek 'klima' which means inclination) was coined by Hipparchus of Nicaea (190–120 BC), a Greek astronomer who divided the then known inhabited world into five latitudinal zones — two polar, two temperate, and one tropical — according to the inclination of the incident sunbeams (in other words, the elevation of the Sun above the horizon). Alexander von Humboldt in his five-volume 'Kosmos' (1845–1862) added to this 'inclination' the effects of the underlying surface of ocean and land on the atmosphere.

Later, the theory of latitudinal and then vertical geographical, including climatic, zoning of land surface received comprehensive treatment and was detailed in the seminal works of Vasiliĭ Dokuchaev (1846–1903). A system of geographical definitions and classifications of the climate was developed, and numerous climatic maps were drawn up showing seasonal and annual variations of mean temperatures, precipitation, atmospheric pressure (reduced to sea level), etc.

Currently we distinguish equatorial, subequatorial, tropical (tradewind), subtropical, temperate, subpolar and polar climatic zones. On land they correspond to particular types of vegetation (or landscapes) — tropical (rain) forests, savannas, subtropical deserts, steppes, deciduous forests, coniferous forests, tundra, and snow–glacial areas. Zoning also correlates with the reflectivity (albedo) of the Earth with respect to solar radiation, which varies from 0.25 in the tropics to 0.6 in the polar regions, and with the heat emission of the Earth, which falls from 0.35–0.40 cal cm^{-2} min^{-1} in the tropics to 0.25–0.20 cal cm^{-2} min^{-1} in the polar regions.

Equatorial and tropical regions are characterized by convective cloudiness and torrential rainfall, so these zones are found to be humid. The subtropical zones are arid. Cyclones in the temperate latitudes carry much precipitation, so these zones prove to be humid again. In the frigid polar regions the air is relatively dry.

For the theory of climate change, however, this approach is not practicable because of two fundamental drawbacks. Firstly, it regards the climate as a kind of stable 'average' state, whose fluctuations are treated as superficial secondary characteristics. Secondly, the atmosphere is considered alone, all by itself.

At the same time, we have already emphasized the sudden and chaotic changeability of the climate, which may render mean climatic maps about as meaningless as the average temperature of patients in a hospital. Because of this, the theory of climate must be constructed from the outset as a statistical theory based on the probability distribution over the phase space of the climate system.

In addition, the climate system cannot be confined to the atmosphere alone because *the atmosphere is not self-sufficient*: its instantaneous state does not determine its further evolution. The climate system must include other layers of the Earth, which interact with the atmosphere.

First of all, this includes oceans and seas, and then the upper (called active) layer of solid earth — mainly the land [sometimes distinguished are layers with frozen water (cryosphere), living matter (biosphere), and the viscoplastic layer of softened rock beneath the lithosphere known as asthenosphere, into which portions of land loaded with heavy continental ice shields may sink to the depth of several hundred meters, or which may alternatively rise to the level of the bottom of the ocean in the zones of spreading on the axes of mid-oceanic ridges].

These blocks of the climate system are far from being coequal. If, for example, we define active layers as those which show seasonal variations, then the average thickness of this layer is 240 meters in the ocean, and 10 meters on dry land. Taking the atmosphere in its entirety, for the mass ratio O:L:A we get 16.4:0.55:1, and for the ratio of integral heat capacities 77:0.5:1.1 (the relative changes in temperature caused by the same change in enthalpy are 0.013:2.0:0.91).

We see that both mechanically and thermodynamically it is the ocean that is the most inertial component in the OLA climate system, so it should be responsible for long-term weather anomalies and climate changes. It must be said that the continental ice caps are even more inertial; we place land second to the ocean because of its ability to accumulate ice shields.

The atmosphere is a low-inertia block which quickly responds to the state of the ocean and serves as an indicator of the state of the OLA system (much like a voltmeter that indicates the voltage across an electric circuit but has almost no effect on its state). The atmosphere, however, is not completely passive: its movements produce wind currents in the ocean, and it carries precipitation that builds up ice shields on land.

The instantaneous state of the atmosphere is referred to as 'weather'. This term can be aptly extended to the instantaneous state of the entire OLA system. This state is defined with a particular set of 'fields' — that is, functions of space coordinates and time. For example, the atmosphere is characterized by the conventional hydrodynamic fields: velocity vector, pressure, density, temperature, entropy, thermodynamically active impurities (TAI) — water in the form of steam, liquid droplets and ice crystals, other greenhouse gases, and aerosols (in the dynamics of the atmosphere a special attention ought to be paid to the phase transformations of moisture and the processes of radiative transfer).

A specific TAI in the ocean is the salt (which is important for the stratification of water density), while the biological processes depend on the so-called biogenic elements contained in the water — oxygen, compounds of carbon, silicon, nitrogen and phosphorus. Specific for the land are the processes of the hydrological cycle — precipitation, evaporation, surface and underground drainage.

All the aforesaid implies that there is nothing mysterious in the dynamics of the climate system. However, the computational difficulties associated with the required resolution in describing the 'fields' on the discrete 'grids' of space – time points are still insurmountable even for present-day computers. Because of this, novel noncomputational ideas are necessary not only for making forecasts of the future evolution of climate system, but also for explaining the climate changes in the past.

One of the most general ideas consists in the transition from the attempts at individual description of the evolution of the 'fields' to the construction of their statistical dynamics treating the fields as a *multicomponent random field*.

Statistical description requires introducing the operation of averaging. Graphs like those in Fig. 2 reveal that spatial averaging, even global averaging, does not destroy the chaoticity of climate oscillations. As regards the time averaging, the period of averaging must be selected if possible in such a way that the mean values are 'statistically stable' — that is, do not show 'level evolution' when the averaging period is varied.

Such possibility does exist if the energy spectrum of the periods of oscillations has a 'window' — that is, a relatively deep and wide minimum; then there will be no evolution of level as long as the period of averaging falls within this window. The composite (Fig. 4) spectrum of oscillations of air temperature in the North Atlantic sector of terrestrial globe, according to Kutzbach and Bryson [20], indicates that such a 'window' embraces periods from several decades to several centuries. To the right of the 'window' is the spectrum of weather changes, and to the left is the spectrum of long-period climate oscillations whose spectral density $s(f)$ grows with a decrease in frequency f as f^{-1} or even faster. A random process with such a spectrum is known as 'red noise' and, unlike the 'white noise' with $s(f) = \text{const}$, is to some extent predictable.

It is certainly more expedient to select the averaging period from the right-hand part of the 'window'; then the averaging can be supported by the accumulated results of instrumental observations. Then the climate may be advantageously defined as follows:

Climate is designated the statistical ensemble of states passed through by the climate OLA system over time periods of several decades.

By statistical ensemble here we mean the set $\mathfrak{A}$ (phase space) of elements a ('weathers') on which the probability measure $P(A)$ is defined; this measure gives for each measurable subset $A \subset \mathfrak{A}$ its probability $P(a \in A)$.

The international meteorological conferences of 1935 in Warsaw and of 1957 in Washington recommended using thirty-year periods for defining the characteristics of the current climate of the atmosphere.

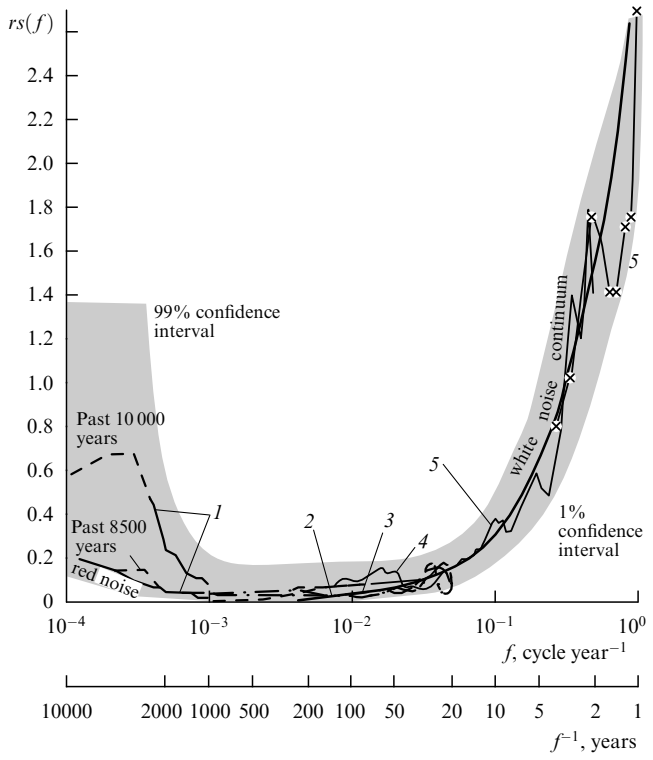

Figure 4. Composite spectrum of oscillations of air temperature in the North Atlantic sector of the terrestrial globe, according to Kutzbach and Bryson [20]: f — frequencies, cycle year^{-1}; $s(f)$ — spectral density; *1* — Central England, paleobotany; *2* — Central England, chronicles; *3* — Iceland, chronicles; *4* — Greenland, by $\delta^{18}O$; *5* — Central England, Manley records [1, 2].

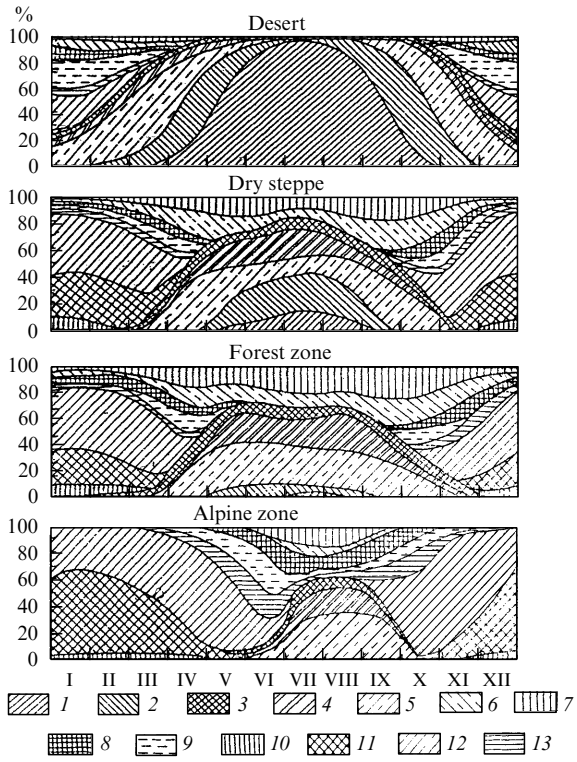

Figure 5. Examples of seasonal oscillations of statistical ensembles of 'weathers' that make up the climates of natural land zones, according to E E Fedorov [21]. Weathers with temperature above 0 °C: *1* — drought-arid; *2* — arid; *3* — cloudy at night; *4* — cloudy in daytime; *5* — slightly cloudy; *6* — cloudy without rain; *7* — rainy; *8* — cloudy. Weathers with temperature going below 0 °C: *9* — slightly cloudy; *10* — highly frosty; *11* — fairly frosty; *12* — moderately frosty; *13* — slightly frosty.

Given the above definition, the complete statistical description of climate would consist in stating all finite-dimensional probability distributions for the values of all 'fields' that characterize the climate system for all possible finite sets of points in space–time. This problem is fairly similar to the problem of turbulence, and differs from the latter only in the number of 'fields' that characterize the system.

Of course, instead of describing the climate of the entire OLA system one may wish to confine the treatment to one of its subsystems — for example, the oceans and seas or a part of them, the atmosphere of the northern hemisphere, the continent or a given territory, etc. Then, however, the description of the climate of the subsystem must include the characteristics of its interaction with other components of the system.

In practice, it would not be feasible to state all the finite-dimensional probability distributions. So, as in the case of turbulence, the treatment is confined to the one-point and two-point distributions, and primarily their first and second moments. Geographical distributions of the mean values of particular characteristics of climate (i.e. their first moments) are pictured in so-called climatic maps.

It is convenient to classify the characteristics of the climate into integral (global), altitudinal distributions (vertical profiles), latitudinal distributions (zonal profiles), nonzonal inhomogeneities, statistical characteristics of time oscillations (short-period, such as turbulence and waves, diurnal, synoptic, seasonal and lasting for several years, whereas the secular variations and those lasting for several centuries and even longer-periodic are regarded as the changes of climate). Historically the most concordant with this definition of climate was the so-called complex climatology of E E Fedorov [21], which treated the climates of natural land zones as the statistical ensembles of the relevant 'weathers' with their seasonal oscillations (even though it lacked the 'sense of globality' and a comprehensive concept of the climate system). Some examples are shown in Fig. 5.

3. Solar climate — the boundary condition for the climate system

The main source of energy for the processes in the climate system of the Earth is incident solar flux. Its intensity I_0 at Earth's mean distance r_0 from the Sun, according to both terrestrial and extraterrestrial measurements, is $I_0 = 1360 \pm 20$ W m^{-2} $= 1.95 \pm 0.03$ cal cm^{-2} min^{-1} (ranging from 1322 to 1428 W m^{-2}) — this corresponds to a total power of radiation emitted by the Sun (solar luminosity) of about 3.83×10^{26} W, and an effective temperature of solar radiation of 5770 K.

Measurements did not reveal any considerable and persistent time variations of the quantity I_0, which came to be known accordingly as the *solar constant*. Satellite-based measurements showed only short-term variations in I_0 with periods of days or weeks and amplitudes of tenths of a percent, apparently associated with the passage of active regions across the surface of the Sun (sunspots attenuate the

light leaving the surface) [22 – 26, 27]. Contrary to the expectations of many authors, no variations in I_0 with the periods of sunspot cycle and the polarity reversal of the heliomagnetic field (about 11.5 years) were discovered. Even if they do exist, such amplitude variations cannot be stronger than 0.1%.

This solar activity, which is an important feature of the solar climate, is apparently caused by the gravitational effects of the planets, which give rise to oscillations in the orbital momentum of the Sun and the tidal motions [28 – 30]. (Recall that according to Newton's law of gravity the orbits of two gravitating bodies are ellipses, one of whose foci coincides with the center of mass of the bodies and not with the Sun, as in the simplified formulation of Kepler's first law.) The main actor is, of course, Jupiter: the center of mass of the system Sun – Jupiter lies outside the Sun, at a distance of about $1.1R_\odot$ from the center of the Sun. It is not surprising then that the periods of sunspot cycle are close to the Jovian orbital period of 11.86 years and the same period of the Sun's orbital motion around the center of mass, which produces gravitational forces in the Sun's depths and eventually generates sunspots. (Note also that the center of mass of the system Sun – Saturn is located at a distance of about $0.6R_\odot$ from the center of the Sun, and that the system Sun – Jupiter – Saturn has a characteristic period of 61 years.)

Quasi-periodical oscillations of solar activity ('the solar cycle') are clearly manifested in emitting the corpuscular 'solar wind' (mainly consisting of protons) and the 'frozen-in' magnetic fields. They produce quite considerable disturbances in the Earth's magnetosphere — magnetic storms, auroras, etc. Their relative contribution to the flux of energy I_0 of solar radiation, however, is very small, and by themselves they hardly cause any significant changes in global weather and climate. It is not surprising therefore that in the climatic spectra we do not see oscillations with the solar cycle period of about 11.5 years [31 – 35].

The total flux of solar radiation energy reaching the Earth is $\pi R_\oplus^2 I_0$, where $R_\oplus$ is the Earth's radius. As the Earth is rotating, in 24 hours this energy is distributed over the entire surface of the Earth $4\pi R_\oplus^2$, and so the mean power of surface irradiation is $I_0/4$: the geometry reduces the incident solar flux fourfold. Observe that the measured power of the internal ('geothermal') heat flux at the Earth's surface is as small as $4.2 \times 10^{13}\,\mathrm{W} \approx 0.03\,\%\ I_0$ (on the continents from $3.8 \times 10^{-2}\,\mathrm{W\ m^{-2}}$ on the ancient shields to $9.2 \times 10^{-2}\,\mathrm{W\,m^{-2}}$ in the regions of contemporary volcanism; in the oceans from $3.8 \times 10^{-2}\,\mathrm{W\,m^{-2}}$ in deep troughs to $3.3 \times 10^{-1}\,\mathrm{W\,m^{-2}}$ on the axes of mid-oceanic ridges). In this case the energy releasing in gravitational differentiation of the Earth's depths and in radioactive decay constitutes respectively 67 and 26% (the balance of 7% comes from the dissipation of tidal energy) — see, for example, our book [36], and McDonald's estimate for the dissipation of tidal energy [37].

Thus, variations in the incident solar radiation and the internal sources of heat are not important for the oscillations in the current climate of the Earth, and the only external factors capable of producing climate oscillations are gravitational forces from other celestial bodies, which disturb the orbital motion and proper rotation of the Earth. All this also applies to other terrestrial planets. (On the major planets internal heat production due mainly to continued gravitational contraction turned out to be greater than the respective solar constants. For the satellites of the major planets with resonant tidal effects, very important is the dissipation of the energy of the tides, which is responsible for such phenomena as sulfur volcanoes on Io, the ocean under the ice on Europe, ice tectonics on Ganimed and Encelad — the seventh satellite of Saturn, etc.).

The surface distribution of *insolation* — that is, the solar flux falling on the surface of the Earth — and the time variations of this distribution are the most important *boundary conditions for the climate system* (the term 'insolation' is universally used in the world literature on climatology). These boundary conditions may be referred to as the *solar climate*. The characteristics of solar climate were first calculated by M Milankovich [38 – 44] (see also Refs [4, 14, 15, 45 – 48]. The instantaneous insolation is given by

$$I_1 = I_0 \frac{r_0}{r} \cos\zeta\,,$$
$$\cos\zeta = \sin\varphi \sin\delta + \cos\varphi \cos\delta \cos\psi\,, \qquad (3.1)$$

where ζ is the zenith angle of the Sun; φ is the geographical latitude of the location; δ is the geocentric declination of the Sun (i.e. the angle between the direction towards the Sun and the equatorial plane of the Earth), and $\psi = 2\pi t/\tau_\odot$ is the hour angle (i.e. the angle between the meridian plane of the location and the plane passing through the Earth's axis of rotation and the Sun, counted westward from the meridian). Furthermore, t is the time; $\tau_\odot$ is the solar day defined as $\tau_\odot^{-1} = \tau^{-1} \mp \tau_0^{-1}$, where τ is the sidereal day (i.e. the period of proper rotation of the planet), and τ_0 is the tropical year (i.e. the time between two consecutive entries of the Sun into the point of vernal equinox), the minus sign corresponding to the same directions of the proper rotation and the revolution around the Sun (i.e. anticipation of equinoxes or positive precession). This equation is only good for the daylight — that is, when $\cos\zeta \geqslant 0$ or $\cos\psi \geqslant -\tan\varphi \tan\delta$ (in the polar regions during the seasons when $\tan\delta \geqslant \cot\varphi$ this inequality holds for any ψ — the Sun never sets). During the night time $I_1 = 0$.

For slowly rotating planets equation (3.1) clearly describes the time variations of insolation in any fixed meridian. In Ref. [45], this is demonstrated for the examples of Mercury and Venus. For rapidly rotating planets it is more convenient to consider the average daily insolation I. In calculating this average, the quantities r and δ may be regarded as quasi-constant, and then we get

$$I = \frac{I_0}{\pi} \left(\frac{r_0}{r}\right)^2 (\psi_0 \sin\varphi \sin\delta + \cos\varphi \cos\delta \sin\psi_0)\,, \qquad (3.2)$$

where ψ_0 is the hour angle of the Sun at sunset (on polar days with nonsetting Sun $\psi_0 = \pi$, and on polar nights with nonrising Sun $\psi_0 = 0$). It will be convenient to go over from the declination of the Sun δ to its planetocentric longitude λ, setting $\sin\delta = \sin\varepsilon \sin\lambda$, where ε is the angle of inclination of the equator of the planet to the plane of its orbit, and to define r and λ as functions of time t using the Kepler and Lacaille equations:

$$E - e\sin E = \frac{2\pi(t - t_0)}{\tau_0}\,, \qquad \cos E = \frac{r_0 - r}{r_0 e}\,, \qquad (3.3)$$

$$\tan\frac{v}{2} = \left(\frac{1+e}{1-e}\right)^{1/2} \tan\frac{E}{2}\,, \qquad v = \lambda - \Pi\,, \qquad (3.4)$$

where E and v are the so-called eccentric and true anomalies, e is the eccentricity of the orbit, t_0 is the time of transit of the perihelion, Π is the planetocentric longitude of the perihelion

(found from heliocentric parameters by solving the appropriate spherical triangles; see, for example, Ref. [45]). Calculations using formulas (3.2)–(3.4) for Earth and Mars were first done by Milankovich himself. For all the planets (except Pluto), the results can be found in Ref. [45]. Apart from the obvious inverse proportionality to the distance squared from the Sun, these results demonstrate strongest dependence on the angle of inclination ε of the planet equator to the orbit plane. Figure 6 illustrates this finding with the examples of Jupiter ($\varepsilon = 3°07'$), Earth ($\varepsilon = 23°27'$) and Uranus ($\varepsilon = 98°$).

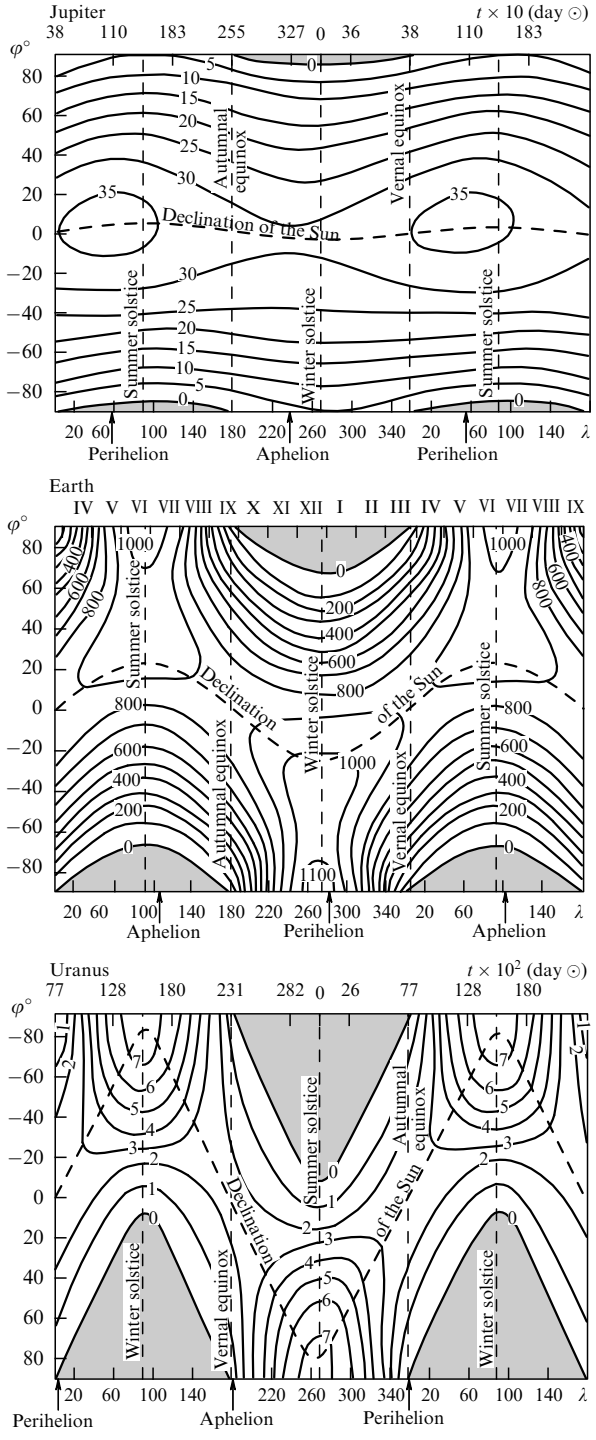

Figure 6. Distributions of average daily insolation I (isolines in units of cal cm^{-2} day^{-1} at $I_0 = 1.946$ cal cm^{-2} min^{-1}) with respect to planetocentric latitudes φ and orbital longitudes λ of the Sun for Jupiter ($\varepsilon = 3°07'$), Earth ($\varepsilon = 23°27'$), and Uranus ($\varepsilon = 98°$) [45]. Vertical dashed lines mark solstices and equinoxes, dashed curves indicate declination of the Sun. Regions of polar night are hatched.

The distribution of daily insolation over the Earth's surface obviously does not depend on the terrestrial longitude and thus exhibits *latitudinal zonality*. Horizontal inhomogeneity of the atmosphere (especially cloudiness) and of the Earth's surface is responsible for the distortion of the latitudinal zonality in the distributions of reflected and absorbed radiation, but this distortion is not too great. Because of this, the zonality of daily insolation leads to the already mentioned approximate longitudinal zonality of the climate.

Apart from the inclination ε, the distribution of daily insolation depends on the eccentricity of the planet's orbit. For example, when it is summer in the northern hemisphere, the Earth passes the aphelion of its orbit, where its distance r to the Sun is the greatest (about 1.52×10^{13} cm), whereas during the summer in the southern hemisphere the Earth passes the perihelion (about 1.47×10^{13} cm). Accordingly, the summer insolation in the southern hemisphere is greater and the winter insolation smaller than in the northern hemisphere. Taken integrally over the year, this asymmetry disappears.

On the equator during the winter solstice (for the northern hemisphere) the daily insolation is 847 cal cm^{-2} day^{-1}, and during summer the latitudinal zonality of insolation is considerably smoothed. At the time of summer solstice, the insolation reaches its maximum value of about 1077 units at the North Pole, while at the same time on the equator it equals 792 units, and exhibits a secondary maximum of 994 units at the latitudes 40–45°, and a secondary minimum of 979 units at the latitudes 60–65°. Such bimodality of meridional distribution of insolation is associated with the duration of the polar day with its nonsetting Sun; this bimodality would disappear if the angle between the equator and the ecliptic was zero.

For $\varepsilon < 45°$ (that is, on all planets except Uranus), the latitudinal circles that form the boundaries of the polar zones wherein days occur with nonsetting and nonrising Sun (polar days and polar nights), lie outside the torrid zone in which days happen with the Sun in the zenith, and since e is small, the insolation at any latitude has annually one maximum and one minimum (counting the polar night for one minimum). Uranus is special in that it rotates practically lying on its side in the plane of its orbit. Roughly speaking, its polar days and nights last for half a year; in the middle of the daylight hemisphere the Sun is near the zenith, and summer and winter alternate twice a year in the equatorial zone — they are relatively more temperate than those in the polar regions.

Integrating the daily insolation (3.2) over the tropical year τ_0 (and assuming that I_0, τ_0, e and ε are quasi-constant), we find the annual insolation

$$W_0 = \frac{I_0 \tau_0}{\pi\sqrt{1-e^2}}\, S(\varphi, \varepsilon)\,,$$

$$S(\varphi, \varepsilon) = \frac{\sin\varphi \sin\varepsilon}{2\pi} \int_0^{2\pi} (\psi_0 - \tan\psi_0) \sin\lambda \, \mathrm{d}\lambda\,,$$

$$\cos\psi_0 = -\tan\varphi \sin\varepsilon \sin\lambda \,(1 - \sin^2\varepsilon \sin^2\lambda)^{-1/2}\,. \qquad (3.5)$$

For those φ and λ for which this expression for $\cos\psi_0$ proves to be less than -1 (i.e. during the polar day) we must set $\psi_0 = \pi$, and when it gives more than 1 (i.e. during the polar

night) we must set $\psi_0 = 0$. Function $S(\varphi, \varepsilon)$ is expressed in terms of elliptic functions. In particular, on the equator it is $(2/\pi)E \sin\varepsilon$, where $E(k)$ is the complete elliptic integral of the second kind, and on the pole it is $\sin\varepsilon$. The ratio of the annual insolation on the equator and on the pole at $\varepsilon < 54°$ is greater than one (on the Earth, where $\varepsilon = 23°27'$, it is approximately 2.5). At $\varepsilon = 54°$ this ratio becomes equal to one, and for Uranus it is less than one (approximately 0.6). The meridional distributions of the average annual insolation W_0/τ_0 are shown in Fig. 7 (on the log scale).

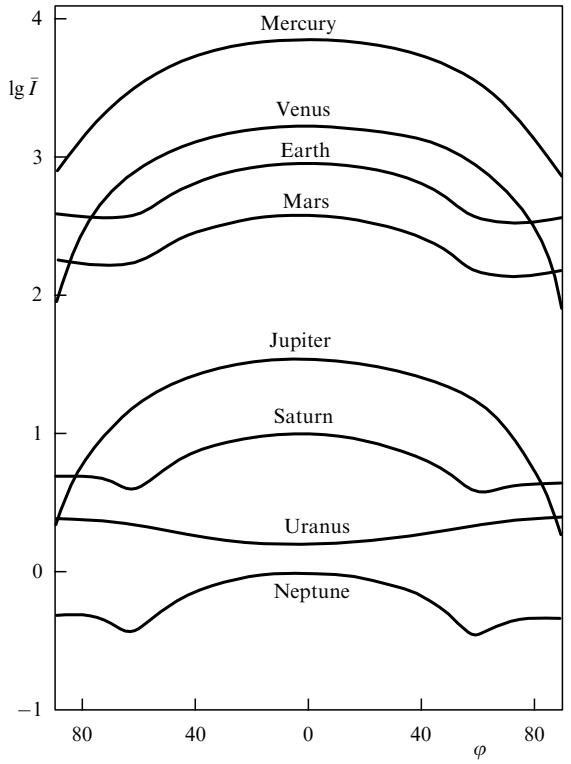

Figure 7. Meridional distribution of the average annual insolation W_0/τ_0 for different planets [45].

Although insolation transforms into the heat supplied to the climate system through the complex mechanism of reflection, absorption and re-emission of radiation, and into the air temperature through an even more complicated equalizing circulation of atmosphere and ocean, the average annual zonal temperatures prove to be approximately linear functions of the annual insolation, whose slope $K = (\delta T/T_{\rm av})(\delta W_0/W_{0\,\rm av})^{-1}$ is the most straightforward indicator of the climate sensitivity to variations of the solar constant. For example, taking for the differences of temperatures δT and insolations δW_0 between the equator and the North Pole the values of 46 °C and 15.03 kcal cm^{-2} month^{-1}, respectively, and for their latitudinal averages $T_{\rm av}$ and $W_{0\,\rm av}$ (corresponding approximately to 39°N) the values of 15.2 °C and 20.06 kcal cm^{-2} month^{-1}, we get $K \approx 0.2$. This means that the change of the solar constant by 1% brings about a change in the climatic temperature of about 0.6°C. Such sensitivity is not too high but is still noticeable.

Observe that the total insolation received at the latitude φ while the Sun traverses the arc of the ecliptic (λ_1, λ_2) equals the insolation received at the latitude $-\varphi$ while the Sun traverses the arc of the ecliptic $(\lambda_1 + \pi, \lambda_2 + \pi)$. This symmetry allows us to confine our further discussion to the northern hemisphere, for which the points $\lambda = 0$, $\pi/2$, π, $3\pi/2$ divide the tropical year into astronomical spring, summer, autumn and winter. In the Arctic zone $\varphi \geqslant \pi/2 - \varepsilon$, the interval of longitudes $(\lambda_*, \pi - \lambda_*)$, where $\sin\lambda_* = \cos\varphi/\sin\varepsilon$, corresponds to the nonsetting Sun (point λ_* occurs in the spring, and $\pi - \lambda_*$ in the summer), and the interval $(\pi + \lambda_*, 2\pi - \lambda_*)$ to the nonrising Sun (point $\pi + \lambda_*$ occurs in the autumn, and $2\pi - \lambda_*$ in the winter); at all other times the Sun rises and sets every day. The values of insolation for spring and summer are the same, and they are the same for autumn and winter. The values of insolation $W_{\rm S}$ for the summer half-year (spring + summer) and $W_{\rm W}$ for the winter half-year (autumn + winter) are given by

$$W_{\rm SW} = \frac{I_0\tau_0}{2\pi\sqrt{1-e^2}}\left[S(\varphi,\varepsilon) \pm \sin\varphi\sin\varepsilon\right]. \tag{3.6}$$

According to Kepler's third law, the year span τ_0 is proportional to $r_0^{3/2}$. As proved by Laplace, correct to the first power of eccentricity e, the perturbations of planet orbits caused by their gravitational interaction do not change the value of r_0, and hence the values of τ_0 and W_0. This means that, down to the same accuracy, these perturbations can only lead to the redistribution of the total insolation W_0 between the seasons and the latitudinal zones. The half-yearly insolations (3.6), however, are not suitable for drawing conclusions about seasonal perturbations, because the lengths of astronomical half-years are not the same: to the accuracy indicated above, $\tau_{\rm S,W} \approx (\tau_0/2)[1 \pm (4/\pi)e\sin\Pi]$. For this reason, Milankovich preferred considering so-called *caloric half-years* defined separately for each latitude φ as equal half-year periods $\tau_0/2$ for which the daily insolation at the latitude φ in the summer half-year every day is greater than the daily insolation at the same latitude on any day during the winter half-year. To the accuracy indicated above, the insolations over the caloric half-years are given by

$$Q_{\rm SW} = \frac{I_0\tau_0}{2\pi}\left[S(\varphi,\varepsilon) \pm \sin\varphi\sin\varepsilon \mp \frac{4}{\pi}\,e\sin\Pi\cos\varphi\right]. \tag{3.7}$$

These functions for the contemporary Earth (1956 epoch) are plotted in Fig. 8. For the visual representation of their disturbances, Milankovich proposed indicating for each latitude φ the so-called *equivalent latitude* $\varphi_1(t)$ found from the equation $Q_1(\varphi_1 0) = Q(\varphi, t)$, so that in the astronomical epoch t the latitude φ receives as much heat from the Sun during the caloric half-year as is currently received at the latitude φ_1. If $\varphi_1 > \varphi$, the latitude φ received less heat in the epoch t than currently, and more if $\varphi_1 < \varphi$.

The effects of other planets enter the equations for perturbations $\delta Q_{\rm SW}$ through the perturbations of three parameters ε, e, and $e\sin\Pi$. For time periods greater than several centuries, these perturbations are represented as trigonometric series calculated even by J Lagrange (1782), P Laplace (1798 – 1825), U Leverrier (1855 – 1878), and later revised by many authors including the recent results of P Bretagnon (1974) and A Berger (1974 – 1977) (see bibliography in Refs [14, 47]).

In Refs [46, 47] we used the calculated results of the Russian astronomers Sharaf and Budnikova [49 – 51] covering the period from 30 million years ago to 1 million years ahead; the series for ε included 48 terms, the leading ones having the amplitudes A and periods τ (in thousands of years)

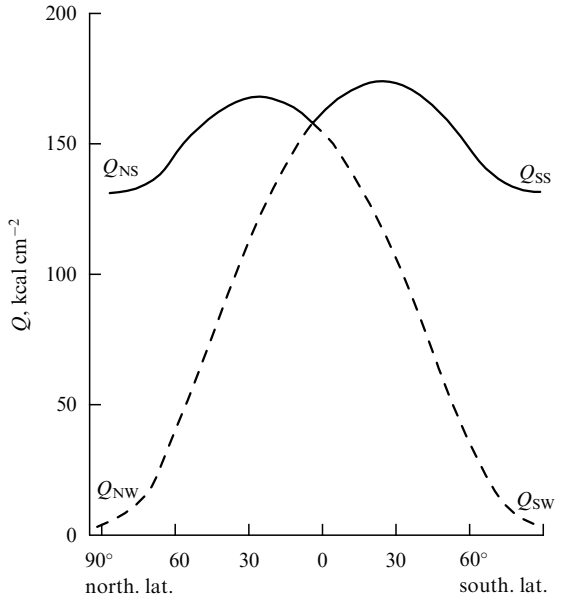

Figure 8. Insolation over caloric half-years for the Earth in the modern epoch (1956): solid curves — summer half-years; dashed curves — winter half-years.

equal to (0.829°; 40.9), (0.168°; 52.5), (0.1400°; 39.5), (0.070°; 29.5), and (0.056°; 28.6); the slope ε varied between 22.07 and 24.57°. The frequency spectrum of these oscillations $fs(f)$, calculated in Refs [46, 47], was unimodal with the maximum occurring near the period $2\pi f^{-1} \approx 41$ thousand years.

The series for e contained 45 terms with the leading values of (10^3 A, τ) being (8.80; 94.6), (7.84; 121.6), (6.19; 99.4), (5.51; 129.8), and (5.01; 1922.8); the eccentricity e varying between 0.0007 and 0.0658. The spectrum of these oscillations turned out to be unimodal, with a very blurred maximum (near the period of about 100 thousand years). The series for $e\sin\pi$ contained 130 members (10^2 A, τ), the leading being (1.83; 23.7), (1.63; 22.4), (1.48; 18.9), and (1.04; 19.1) with the precession periods; this parameter varied from -0.07 to $+0.03$. The spectrum of these oscillations was bimodal with narrow maxima at the precession periods of 23 and 19 thousand years, while the period of secular oscillations of eccentricity about 100 thousand years was not manifested in this spectrum.

One may assume that cold summer half-years (and respectively, warm winter half-years) facilitate the growth of glaciers and then the climate gets colder — it seems to be the outcome of positive feedback rather than cause and effect. For this reason, and also taking into account the fact that the alternate appearance and recession of glaciation during the Quaternary Period of the Earth's geological history (Pleistocene) was especially marked at the temperate latitudes of the northern hemisphere around $\varphi = 65°$N, Milankovich selected for their representation the equivalent latitudes $\varphi_1(65°\text{N}, t)$. According to calculated results of Sharaf and Budnikova [49–51], over the period $(-30, +1)$ million years these equivalent latitudes varied between 58 and 79°, which is quite considerable. The results of these calculations for the period $(-1, +1)$ million years are given in Fig. 9, which shows seven periods of cold spell with $\varphi_1 \geqslant 68°$N (blackened in the diagram). They are in perfect agreement with the paleographic data concerning the ice age chronology in Alps: the three Danube stages and the glacial periods of Günz-1, 2, Mindel-1,2, Riss-1, 2, and Würm-1, 2, 3.

A lot of information is lost, however, when the treatment is only confined to the equivalent latitudes $\varphi_1(65°\text{N})$. So in Refs [46, 47] we plotted (in the Laplacian approximation) isolines of insolation anomalies for the summer caloric half-years in the northern and southern hemispheres in the coordinates latitude–time over the period $(-1, +0.05)$ million years. We found that the most intense anomalies in a given season have the same sign for the entire Earth; for a given hemisphere they change the sign upon transition from

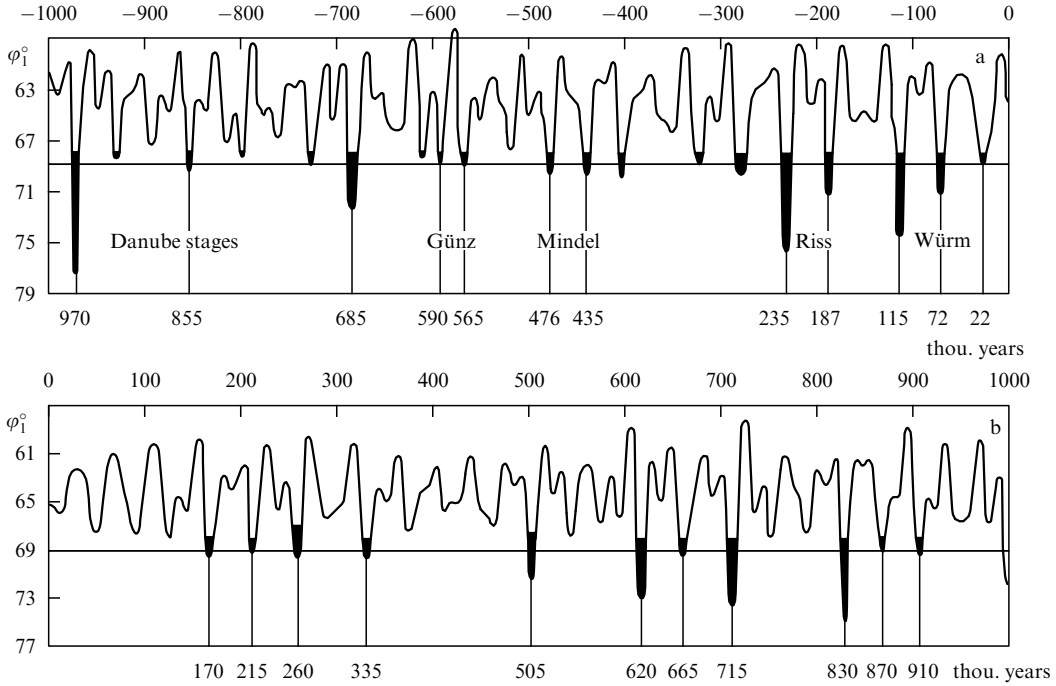

Figure 9. Equivalent latitudes for Q_S (65° N) for the past million years (a) and for a million years ahead (b), according to Sharaf and Budnikova [51].

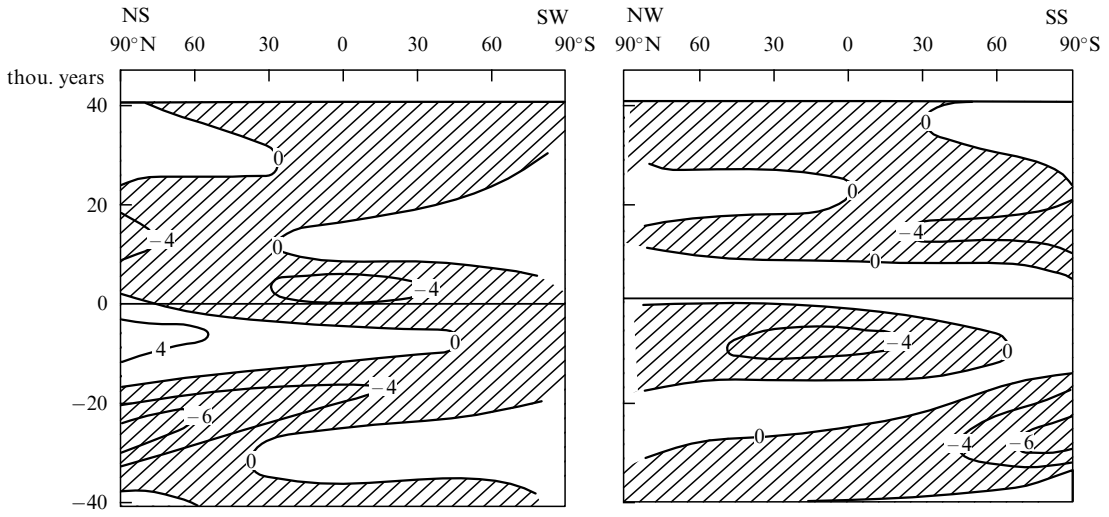

Figure 10. Isolines of insolation anomalies for caloric half-years (in kcal cm^{-2}) over the period (−40, +40) thousand years [46, 47]. Regions of negative anomalies are hatched.

summer to winter half-year and are quasi-periodic with a period of about 20 thousand years. Somewhat less intense anomalies were found at the high and temperate latitudes of the summer hemispheres; they have the same sign in the summer half-year both in the northern and southern hemispheres and are quasi-periodic with a period of about 40 thousand years. For illustration, in Fig. 10 we reproduce the isolines of insolation anomalies over the period (−40, +40) thousand years.

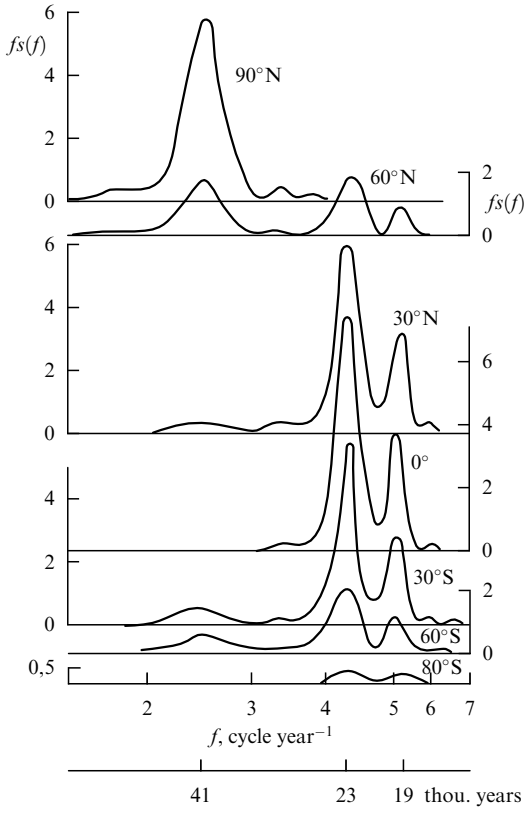

Figure 11. Spectra of insolation oscillations δQ_{NS} and δQ_{SW} at different latitudes [46, 47].

Using these results, we calculated the spectra of insolation oscillations at various latitudes (Fig. 11). They exhibit a peak at the period of 41 thousand years, and a double peak at the periods of 23 and 19 thousand years (the latter is a little smaller; observe that in the Laplacian approximation, which disregards variations of the eccentricity squared $\delta(e^2)$, the peak at the period of 100 thousand years disappears). The peak at 41 thousand years is highest on the summer pole; it decreases towards the equator and almost flattens out at the latitudes of 20 – 0°; then it grows again to a small height at 40 – 60°, and rapidly disappears towards the winter pole. The double peak at 23 and 19 thousand years is highest in the equatorial zone, and disappears towards the poles.

The discovery (in 1976) of spectra with similar peaks in the layer alternation of deep-sea oceanic sedimentation served as conclusive evidence that the climate oscillations inherent in the phases of glacial advances and retreats in the Quaternary Period of the geological history of the Earth were really caused by oscillations in the distribution of insolation, triggered by perturbations in the orbital motion and rotation of the Earth due to the gravitational forces exerted from the side of other planets (that is, insolation makes up a very strong boundary condition for the climate system). In this sense, planetary motion effectively 'controls' the most prominent climatic changes (with periods of tens of millennia).

Milankovich's astronomical theory of climatic changes ranks as the most important achievement in the theory of climate in the current century, which is the reason why we have discussed it first and in so much detail. Its predictions, such as those illustrated in Figs 9 and 10, are quite credible — so while a forecast for the next million years is of little concern for anyone, the knowledge of natural climatic trends for the next few thousand years may be of practical use today, when mankind is learning the art of scientific global self-organization. Such predictions are well worth further detailing and refining, with the Laplacian approximation being replaced with more advanced approaches — for example, in the spirit of P Bretagnon [52] and A Berger [53]. According to Fig. 10, the Earth is currently passing through an interglacial period, and the next minimum of insolation covers the coming period

of 20 thousand years, will reach a peak in 10 thousand years, and will have a shape similar to the preceding minimum (Würm-3) with somewhat lesser intensity.

At the same time, the 'power' of insolation as a boundary condition for the climate system is still deficient. The astronomical theory, while explaining the glacial periods of the Pleistocene, does not account for their absence in most of the other geological epochs, although the oscillations in insolations analogous to those in the Pleistocene would seem to have been always present. This should mean that most of the time the climate system is in the states not responsive to the oscillations of insolation, and only occasionally comes to state where a resonance takes place.

In other words, the periods of the climate system's natural oscillations ought to depend on certain parameters in such a way that for most of geological time they were much different from the periods of the driving force (oscillations in insolation), and only occasionally became close to the latter so that the system responded in resonance.

Such parameters may be the characteristics of the average temperature background of the geological epoch — for example, there is no resonance when the average temperature is above 13 °C, but resonant oscillations set in when the average temperature falls below 10 °C. Such a hypothesis was put forward by P Woldstedt as early as 1954 [54]. It fits in with the factual evidence on a gradual decrease in the temperature background over the Cenozoic Era (the last 67 million years). This decrease in the temperature background could be caused by the movement of continents, which brings about a change in the relative area of the continents in the equatorial zone and in the polar regions.

This implies that the astronomical theory must be augmented by the study of the resonant properties of the climate system and their changes on the geological time scale.

Oscillations in insolation (3.7) on Mars are even more prominent than on the Earth. As a matter of fact, Mars is the second planet (after the Moon) scheduled for a manned mission, so knowledge of its climate may come in handy. Calculations of insolation oscillations for Mars were done by Murray and Ward with colleagues [55–58], and by Sharaf and Budnikova [59–60] with our refinements similar to those shown in Figs 10, 11. It was found that variations of the parameters ε and e on Mars are greater than those for the Earth by factors of five and two, respectively (owing to the greater influence of Jupiter and Earth). The spectrum of the oscillations of ε has a broad maximum at the period of 117 thousand years; that of e has a very broad maximum at the period of 95 thousand years, and the spectrum of $e \sin \Pi$ has a narrow maximum at the period of 52 thousand years.

According to calculations over the time interval $(-1, +0.05)$ million years, the oscillations in insolation for the caloric half-years δQ_{SW} on Mars are by no means small. For example, on the summer poles they are sometimes as large as $+37$ kcal cm^{-2}, or 32.5% of the mean insolation (on the Earth they only reach ± 6 kcal cm^{-2}, or less than 5% of the mean insolation). The contribution of $\delta\varepsilon$ to the oscillations in seasonal insolation on Mars is quasi-periodic with a period of about 117 thousand years; it is well pronounced at the high latitudes of the summer hemispheres and has, as a rule, the same sign during the summer half-years in the northern and southern hemispheres. The contribution of $\delta(e \sin \Pi)$ is quasi-periodic with a period of about 52 thousand years, it reaches its maximum on the equator, in any given season it has the same sign on the entire planet, and changes its sign in a given hemisphere upon transition from a summer to winter half-year. When the minima of these two contributions coincide, we have the epochs of minimum insolation. According to calculations similar to those illustrated in Fig. 10, such epochs occurred, in particular, 50 and 150 thousand years ago. Currently Mars is passing through a moderately negative insolation anomaly, and a positive anomaly will develop approximately 30 thousand years from now.

When considering the response of the climate system of Mars to insolation anomalies, one should recall that (1) the atmosphere of Mars is very thin (its surface pressure on average is 0.6% of atmospheric pressure at sea level on the Earth, with variations from 0.2 to 1.0%) and consists mainly of carbon dioxide; (2) the Martian geometric figure is 'unicellular' — its 'oceanic' northern hemisphere (bounded by the great circle inclined at 35° to the plane of the equator) is on average 2 kilometers lower than the 'continental' southern hemisphere; (3) Mars has white polar caps, of which the southern grows as large as 1.5 million sq. km (reaching 57°S) in winter, and disappears in summer. The northern cap grows as large as 1.1 million sq. km and survives in summer. The caps are apparently about 2 kilometers thick, and are stratified with layer thickness of about 30 meters.

Since the temperature on the surface of the polar caps was measured to be low as -125 °C (below the freezing point of carbon dioxide), the winter advance and the summer retreat of polar caps are interpreted as freezing over and evaporation of CO_2. This was confirmed by one of the best observational experiments of the 20th century — the measurements of seasonal variations in the partial pressure of carbon dioxide in the atmosphere of Mars, performed by the landing modules of 'Viking 1' and 'Viking 2' space missions (see Fig. 12). The deepest minimum of pressure on the 120th day of measurements in this diagram corresponds to the end of winter on the southern polar cap, the maximum of partial pressure corresponds to the winter solstice, the minimum on the 430th day corresponds to the freezing out of CO_2 on the northern cap before the vernal equinox. The water component of the polar caps may be regarded as the effect of the 'glacial period' at the minimum of insolation, like the numerous traces of water flows — dry beds of meandering rivers, extensive ravine systems, etc.

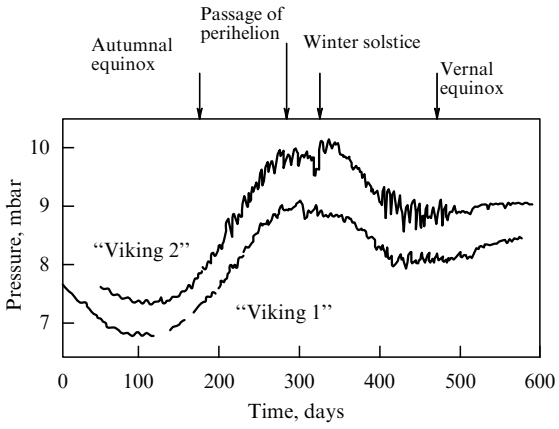

Figure 12. Seasonal variations of partial pressure of carbon dioxide (CO_2) in Martian atmosphere according to measurements from landing stages of Viking 1 and 2.

4. Similarity theory for 'horizontal' processes

The ultimate goal of the theory of climate consists in charting the temperature field in the climate system with due account for its time oscillations (followed by the definition of other climate-related fields) from the given boundary condition — the insolation field — and from the characteristics of the climate system per se, such as the masses and compositions of atmosphere and ocean, the properties of their components (heat capacity, radiation absorption coefficient, etc.), mechanical properties of ice, etc.

This task can be split in two. One part of the problem consists in finding the global (horizontal) inhomogeneities of the temperature fields, produced by the varying amounts of insolation in equatorial and polar zones with due account for the smoothing effects of the large-scale motions caused by temperature differences and the corresponding heat exchange in atmosphere and ocean. Such 'horizontal' processes are well described by G S Golitsyn's similarity theory of circulation in planetary atmospheres.

The other part of the problem concerns the definition of the vertical inhomogeneities of the temperature field, including the 'greenhouse effect', created on the Earth (whose atmosphere is almost completely transparent for the bulk of the energy of solar radiation) through the heating of its surface and the smoothing effects of vertical heat exchange through the thermal convection (vertical transfer of ordinary heat and the latent heat of evaporation transferred by water vapor) which predominates in the lower part of the atmosphere, as well as the radiative transfer of proper thermal radiation produced by the Earth's surface and the atmosphere, which dominates in its upper layers.

The theory ought to provide a general-terms description of the main features of the current climate (as well as climates of the past), which is the purpose of the simplified phenomenological theories, such as the similarity theory, as well as proposing methods for predicting its future evolution, based presumably on sufficiently detailed numerical simulations of the climate system.

Embarking on the presentation of similarity theory, we start by noting that the first of the proper characteristics of the climate system we need is the planetary albedo A — the fraction of incident radiation reflected by the planet, averaged both over the surface of the planet and over the spectrum of solar radiation (the greater A, the less absorbed solar radiant heat, and, other conditions being equal, the colder the climate). Then, from the condition of equilibrium between the assimilated (absorbed) solar flux $q = q_0/(1 - \mathrm{A})$, where $q_0 = I_0/4$, and the emitted (outgoing) long-wave radiation flux of the planet $\sigma T_{\mathrm{eff}}^4$, we find the *effective radiation temperature* T_{eff}:

$$T_{\mathrm{eff}} = \left(\frac{q}{\sigma}\right)^{1/4} \tag{4.1}$$

($\sigma \approx 5.67 \times 10^{-8}\,\mathrm{W\,m^{-2}\,K^{-4}}$ is the Stefan – Boltzmann constant, which sometimes is corrected by a factor a little less than one to account for the fact that the emissivity of the climate system differs from that of a blackbody). According to the measurements (including the satellite-based measurements of recent decades), the Earth has $A \approx 30\%$, and from Eqn (4.1) we get $T_{\mathrm{eff}} \approx 255$ K. By Planck radiation formula, the spectral maximum of blackbody emission occurs at the wavelength $\lambda_{\max} = ch/xk_{\mathrm{B}}T_{\mathrm{eff}}$, where c is the speed of light, h and k_{B} are the Planck and Boltzmann constants, and x is the root of equation $x = -\ln(1 - x/5)$, so that for the Earth we get $\lambda_{\max} \approx 12$ μm.

The temperature 255 K is observed in the terrestrial atmosphere at the altitude of about 5 kilometers. In the lower 10-kilometer layer of the atmosphere the temperature, on the average, decreases with the altitude (because the solar radiation is weakly absorbed by the atmosphere, so it reaches the Earth's surface and heats it; at the same time, the long-wave radiation emitted by the surface is strongly absorbed in the lower atmosphere and also heats it). According to many years of temperature measurements, the average temperature T_{s} of the air surface layer (at the height of the instrument booth) is close to 288 K. The ratio $T_{\mathrm{eff}}/T_{\mathrm{s}} \approx 0.89$ characterizes the temperature stratification of the lower atmosphere. The temperature difference $T_{\mathrm{s\,eff}} = T_{\mathrm{s}} - T_{\mathrm{eff}} \approx 33$ K is known as the greenhouse effect (hothouse, solarium — all these comparisons seem to be not quite to the point, because greenhouses, hothouses or solaria all have glass panes in the ceiling that prevent mixing of inside and outside air). Other conditions being equal, the greater the greenhouse effect, the warmer the lower layers of the atmosphere.

For other planets the values of A and T_{eff} are as follows (see Table 1).

Table 1.

Planet	A, %	T_{eff}, K
Mercury	9	435
Venus	77	228
Mars	24	211
Jupiter	42	109
Saturn	50	76
Uranus	50	57
Neptune	50	46
Pluto	40	32

Observe that Venus is 'twice paradoxical'. First, is receives almost twice as much insolation as the Earth, so its atmosphere should apparently have been much warmer. But the albedo of Venus is tremendous (much like that of snow — this is why Venus is the third brightest object in the sky, exceeded only by the Sun and the Moon). Now we know that such high reflectivity A is due to a very thick layer of dilute sulfuric acid mist at the altitudes of 48 to 67 kilometers, containing 100 – 200 droplets 2 – 3 μm in diameter per cubic centimeter. Owing to the high albedo, Venus absorbs less solar radiant heat than the Earth, and the value of T_{eff} is smaller. Secondly, however, in spite of this the lower atmosphere (including the mist) is very hot: $T_{\mathrm{s}} \approx 735$ K, and then because of the high density of the atmosphere of carbon dioxide (the pressure at the surface is 91 atmospheres), the greenhouse effect is enormous: $T_{\mathrm{s\,eff}} \approx 507$ K (this points to the limitations of the terrestrial 'albedo mechanism' — the negative feedback between albedo and climatic temperature).

For Mars, the effective temperature was found to be considerably above the freezing point of CO_2, so a carbon dioxide atmosphere is quite feasible, which is indeed found (95% CO_2). As indicated above, the freezing out of CO_2 only occurs on the winter polar caps (see Fig. 12). As regards Jupiter, Saturn, Uranus, and Neptune, direct measurements of their infrared emission spectra from space probes Pioneer and Voyager yielded the values of the respective effective temperatures of 130, 95, 58 and 56 K — considerably higher

than the values in our table, calculated from Eqn (4.1) which only takes into account the absorbed insolation (only in the case of Uranus is the discrepancy small). This implies that, apart from insolation, these planets have internal sources of heat, and so the absorbed radiant heat q must be supplemented by the comparable and even greater amount of the internal 'planetothermal' heat flux q_i.

As indicated above, the theory of climate must first of all offer the possibility of calculating the climatic temperatures from given insolation (and internal heat sources). In this case equation (4.1) may be regarded as the ultimate simplification of the climate theory, which takes into account only one characteristic of the climate system — its albedo. To some extent constructive, such a theory is certainly not good enough, so Golitsyn [61–64] developed a more advanced similarity theory for the circulation of planetary atmospheres, assuming that the global characteristics of such circulation are determined by seven dimensional 'external parameters': the quantities q and σ, which enter Eqn (4.1), radius a and angular velocity of rotation ω of the planet, the mass of the unit column of the atmosphere M, the pressure $p_s = Mg$ at its lower boundary (where g is the acceleration due to gravity), the specific heat capacity c_p of the air, and the dimensionless parameter μ — the relative molecular mass of the air, which only enters the equations through $R/\mu = c_p - c_V$, where R is the gas constant, or, which is equivalent, through the velocity of sound $c_{\text{eff}} = [\varkappa(R/\mu)T_{\text{eff}}]^{1/2}$, where $\varkappa = c_p/c_V$. If air is regarded as a mixture of ideal gases with molar concentrations s_c and specific heats c_{pc}, then $c_p = \Sigma s_c c_{pc}$, and $(\varkappa - 1)^{-1} = \Sigma s_c(\varkappa_c - 1)^{-1}$.

Since there are only four independent dimensions (length, time, mass, and temperature), the seven dimensional external parameters may be used for constructing three independent dimensionless combinations (similarity criteria):

$$\Pi_\omega = \frac{a}{2L} = \frac{\omega a}{c_{\text{eff}}} \qquad \left(L = \frac{c_{\text{eff}}}{2\omega}\right),$$

$$\Pi_g = \frac{H}{a} = \frac{c_{\text{eff}}^2}{\varkappa g a} \qquad \left(H = \frac{c_{\text{eff}}^2}{\varkappa g}\right),$$

$$\Pi_M = \frac{\tau_p}{\tau_{\text{eff}}} \qquad \left(\tau_p = \frac{a}{c_{\text{eff}}}\,; \quad \tau_{\text{eff}} = c_p M \frac{T_{\text{eff}}}{q}\right). \tag{4.2}$$

The criterion Π_ω may be regarded as the rotational Mach number, and L as the scale factor of the synoptic atmospheric processes; if ω is so small that $L > 2a$, like on Venus, then one should assume $L = 2a$ and $\Pi_\omega = 1/4$. According to Golitsyn's estimates, Π_ω is of the order of 10^{-2} for Mercury and Venus, 10^0 for Earth and Mars, and 10^1 for the large planets, and may be used as the basis for classification of the atmospheric circulation on these planets. In the expression for Π_g, the quantity H is the so-called thickness of the uniform atmosphere. This parameter is small for all planets (of the order of $10^{-3}-10^{-4}$), so one could expect self-similarity with respect to this parameter. In the expression for Π_M, the quantities τ_p and τ_{eff} are the relaxation times for perturbations of pressure (or density) and temperature relaxation to the local thermal equilibrium. If, by convention, the parameters ω, g, and M only enter the equations of similarity theory through the criteria (4.2), then any characteristic F of the atmospheric circulation in our similarity theory ought to be expressible as

$$F = \sigma^{n_1} q^{n_2} c_p^{n_3} a^{n_4} \Psi_F(\Pi_\omega, \Pi_g, \Pi_M)\,, \tag{4.3}$$

where Ψ_F is a certain universal dimensionless function of the similarity criteria, and the exponents $n_1, \ldots, n_4$ are selected from the considerations of correct dimensionality for F. Using such formula for the total kinetic energy of the atmosphere $E = (1/2)(4\pi a^2 M)U^2$, where U is the rms velocity of atmospheric motions, one may prove that the energy criterion Π_M differs from the Mach number squared $(U/c_{\text{eff}})^2$ only by the coefficient $2\pi(\varkappa - 1)^{1/2}\Psi_E^{-1}$. It is obvious that the parameter Π_M is also small.

Now we introduce the typical time scale of the synoptic processes $\tau_s = L/U$ and define the effective rate of generation of kinetic energy $\varepsilon = E/(4\pi a^2 M\tau_s) = U^3/2L$ in the processes. This formula for ε completely corresponds to the similarity theory of A N Kolmogorov. The quantity ε is obviously equal to $\eta q/M$, where η is the efficiency of the atmospheric 'heat engine', which converts the absorbed heat into mechanical energy of atmospheric motions. This engine is far from the ideal cycle, so its efficiency differs from $\delta T/T_s$ (where δT is the temperature difference between the equator and pole) by a factor k considerably less than one. We shall refer to the quantity $\theta = kT_{\text{eff}}/T_s$ as the 'utilization coefficient'. Then the equation for the specific energy of the atmosphere can be written as

$$\frac{U^3}{2L} = \theta \frac{\delta T}{T_{\text{eff}}} \frac{q}{M}\,. \tag{4.4}$$

In order to define δT, it ought to be supplemented by the simplified equation of meridional heat transfer

$$c_p M U \frac{\delta T}{\pi a/2} = q\,. \tag{4.5}$$

From these two equations it is easy to find δT and U and then E, Ψ_E, ε, η, etc. In particular, we find that $\Psi_E = (1/2)(2\pi)^{3/2}\theta^{1/2}\Pi_\omega^{-1/2}$. It follows that the total kinetic energy E of the atmosphere does not depend explicitly on its mass. At first sight this may be surprising, but then the common sense suggests that a given (thermal) action can drive a heavy atmosphere only to much slower velocities than it could a subtle one. All other parameters show explicit dependence on M: U, δT, and η vary as $M^{-1/2}$, and ε as $M^{-3/2}$.

The possibility remains, however, that the quantity E (and also $M^{1/2}U$, $M^{1/2}\delta T$, $M^{1/2}\eta$, $M^{3/2}\varepsilon$, and $M^{-1/2}\tau_s$) exhibits implicit dependence on M — through the 'utilization coefficient' θ. As presented here, however, the similarity theory does not predict this dependence. It is therefore incomplete and is not capable of predicting the surface-layer temperature T_s and hence the greenhouse effect $T_{s\,\text{eff}}$: equations (4.1) for the generation of kinetic energy and (4.2) for the meridional turbulent heat transfer in the atmosphere are not sufficient for this purpose, and they must be supplemented with additional equations or at least with the decisive parameters inherent in them. We shall return to this issue in Section 5. Here we are going to refer briefly to two works that add detail rather than scope to the similarity theory under discussion.

In our work with Zilitinkevich [65], in addition to the latitude-average value of the absorbed solar flux q, which enters Eqn (4.1), we used the difference δq between solar fluxes on the equator and the pole, which was substituted in place of q into Eqns (4.1) and (4.2), which up to fixed coefficients then become $\varepsilon \sim (\delta T/T)\delta q \sim U^3/T$ and

$TU\delta T \sim \delta q$. Hence we get the relations

$$U \sim q^{-1/16}(\delta q)^{1/2}, \quad \delta T \sim q^{-3/16}(\delta q)^{1/2},$$
$$\varepsilon \sim q^{-7/16}(\delta q)^{3/2}. \qquad (4.6)$$

These formulas describe fairly well the seasonal variations of atmospheric circulation on the Earth. Indeed, we will assume that in the summer hemisphere q is $1+\alpha$ times greater than its average annual value, and the additional flux αq falls mainly on the polar region, so that coefficient $1-\alpha$ appears before δq. According to astronomical data, on the day of the summer solstice $\alpha = 0.33$, and on the day of the winter solstice $\alpha = -0.39$. Then, with the average annual values $U = 20\,\mathrm{m\ s^{-1}}$ and $\delta T = 60\,^\circ\mathrm{C}$, equations (4.6) give the kinetic energies 3.9×10^{20} and 7.1×10^{20} J, and the temperature differences 40 °C and 74 °C for summer and winter in the southern hemisphere, respectively, in very good agreement with the empirical data.

This success of formulas (4.6) suggests that they could be applied to conjectural situations. For example, if we increase the solar constant by a factor of $1+\alpha$ or arrange artificial sources of heat along the equator with a power of αq per unit area of the entire Earth's surface, then we have $q \sim 1+\alpha$ and $\delta q \sim 1+\alpha$. If we evenly distribute these thermal sources over the entire Earth's surface, then $q \sim 1+\alpha$ but δq will not change. If we place these sources on one of the poles in this hemisphere, we get $q \sim 1+\alpha$ and $\delta q \sim 1-\alpha$ (a similar effect could be achieved by reducing the albedo of the arctic zone, but this effect would be small: if, for example, we decrease the albedo from 0.8 to 0.3, then the local heat flux to the Arctic would increase by $2.5\,q$, but being recounted to the unit area of the entire Earth's surface this only amounts to $\alpha \approx 2.5/40 \approx 0.06$ — as little as one-sixth of the seasonal variations). Finally, if the sources of heat with a power of $\alpha q/2$ are placed on both poles, we get $q \sim 1+\alpha$ and $\delta q \sim 1-\alpha/2$.

When $\alpha = 0.1$, the increments of all variables in Eqn (4.6) are small, and so from the standpoint of our simplified theory any noticeable change in the global climate would require artificial sources of heat with a power at least of the order of $0.1\,q$ (that is, of order 10^{13} kW, which is equivalent to the combustion of 2 megatons of TNT every second). In principle, this is only possible through a very dramatic reduction of the global albedo.

In Refs [66–68], the similarity theory was further detailed by supplementing the atmospheric meridional heat flux q_a, described by the left-hand side of Eqn (4.5), with the oceanic flow $q_\mathrm{w} = (2/3)(2Q)$, where Q is the vertical heat flux from atmosphere to ocean at low latitudes, and from ocean to atmosphere at high latitudes (and 2/3 is the relative share of the Earth's area covered by the oceans). This allows the inclusion of the global interaction between atmosphere and ocean in the evaluations of climatic characteristics. The quantity Q was found from the formulas of the theory of a small-scale (local) interaction of atmosphere and ocean:

$$Q = c_\mathrm{w}\rho_\mathrm{w}K\frac{\delta T_\mathrm{w}}{h}, \qquad K = \alpha_\mathrm{w}u_*^2\left(\frac{\delta U_\mathrm{w}}{h}\right)^{-1}, \qquad (4.7)$$

where K and K/α_w are the kinematic coefficients of turbulent heat conductivity and viscosity, respectively, $u_* = [c_\mathrm{f}(\rho_\mathrm{a}/\rho_\mathrm{w})U^2]^{1/2}$ is the velocity of friction in the ocean ($c_\mathrm{f} \sim 10^{-3}$ is the coefficient of sea surface friction), $\delta T_\mathrm{w} \sim \delta T$ and δU_w are the typical vertical gradients of the temperature and flow velocity in the upper active layer (of thickness h) of the ocean; subscript w stands for 'water'. This gives us a new dimensionless criterion which is additional to those in Eqn (4.2): $\Pi_Q = (q_\mathrm{w}/q_\mathrm{a})(\delta T/\delta T_\mathrm{w})^{2/3} \approx 0.4$.

Observe also that K depends on the so-called dynamic Richardson factor Rf — the ratio of the work by the buoyancy forces to the work by the Reynolds stress: $K = u_*^2(\alpha_\mathrm{w}\mathrm{Rf}\,h/\beta\delta T_\mathrm{w})^{1/2}$, where $\beta \approx 0.2\,\mathrm{cm\ s^{-2}\ K^{-1}}$ is the buoyancy parameter of the sea water. The values of α_w and Rf in the ocean are small: $\alpha_\mathrm{w}\,\mathrm{Rf} \approx 5 \times 10^{-4}$. Then, with $u_* = 1\,\mathrm{cm\ s^{-1}}$, $\delta T_\mathrm{w} = 27\,^\circ\mathrm{C}$, and $h = 300$ m, we get $K \approx 5/3\,\mathrm{cm^2\ s^{-1}}$, and the vertical mass flow on the surface of the ocean is $\beta Q/gc_\mathrm{w} = 9.6\,\mathrm{g\ cm^{-2}\ year^{-1}}$, in fairly good agreement with the empirical estimates. Finally, recalling that h increases in the cold season owing to the involvement of the deeper water layers in the convective upper layer of the ocean, we may set $h \sim (K\tau)^{1/2}$, where τ is the annual period. To achieve agreement with the previous estimates, the numerical coefficient in this expression should be made equal to 4.

Having set T_s and calculated δT, we can find the air temperatures on the equator $T_\mathrm{E} = T_\mathrm{s} + (1/3)\delta T$ and at the pole $T_\mathrm{p} = T_\mathrm{s} - (2/3)\delta T$, and set $\delta T_\mathrm{w} = T_\mathrm{E} - \max(T_\mathrm{p}, T_\mathrm{f})$, where T_f is the freezing point of water. For example, in the Mesozoic Era both poles were most likely found in the open ocean, and there was no perennial ice cover in the polar zones, so the global albedo of the Earth was somewhat smaller than today. If we assume that q was 4% greater than today, then T_eff (and hence probably T_s) was 3 °C higher than today, also $\delta T = 31\,^\circ\mathrm{C}$, and T_E and T_p are, respectively, 1 °C and 6 °C higher than today — hence the absence of perennial ice.

During the Carboniferous–Permian glacial epoch, the south pole was located on Gondwanaland, and the north pole apparently in the Pacific ocean. If, in the first approximation, we evaluate the climates of the southern and northern hemispheres separately, then to the southern hemisphere we may ascribe the value of $q_\mathrm{w} = 0$ and, say, albedo of 0.37 (20% are covered by ice with albedo 0.8, and 80% of ice-free land with albedo 0.26). Then T_eff (and apparently T_s) will be 7 °C below the current value, $\delta T = 35\,^\circ\mathrm{C}$, $T_\mathrm{E} = 293$ K, and $T_\mathrm{p} = 258$ K. In the northern hemisphere, however, if we take the Mesozoic $\delta T = 31\,^\circ\mathrm{C}$, we get the temperature in the Arctic close to what it is today: $T_\mathrm{p} = 293 - 31 = 262$ K.

5. 'Vertical' processes, greenhouse effect, and ozone holes

The primary response of the climate system to the action of a given boundary condition — insolation — consists of scattering, reflection, absorption, and re-emission of radiation. Absorption leads to heating, re-emission is determined by the temperature — this creates a linkage between the fields of radiation and the temperature.

In the calculation of the characteristics of these processes, we may approximately regard the field of radiation in the climate system as nonpolarized, and describe it by just one Stokes parameter — the *spectral intensity of radiation* $I_\lambda(\mathbf{x}, \mathbf{n}, t)$, where $\mathbf{x}$ is the space coordinate, and $\mathbf{n}$ is the unit vector in the direction of propagation of electromagnetic waves, so that the vector integral with respect to the solid angles, $\mathbf{F}_\lambda(\mathbf{x}, t) = \int I_\lambda \mathbf{n}\,\mathrm{d}\Omega(\mathbf{n})$, defines the spectral radiant flux, and $\mathbf{F}(\mathbf{x}, t) = \int \mathbf{F}_\lambda\,\mathrm{d}\lambda$ is the integral *radiant flux* (the integral over the values of $\mathbf{n}$ from the upper hemisphere gives the upward flux $\mathbf{F}\uparrow$, and from the lower hemisphere the downward flux $\mathbf{F}\downarrow$).

The climate system may be approximately regarded as a locally plane-parallel medium, in which the direction **n** is conveniently referred to the vertical direction — that is, characterized by the zenith angle ϑ and azimuth ψ; then we consider I_λ as a function of λ, altitude z above the Earth's surface, and angles ϑ and ψ (the dependence on the horizontal coordinates and the time is parametric, through the characteristics of the medium). As is known, this function must satisfy the equation of radiation transfer (see Refs [69–74])

$$\cos\vartheta\ \frac{\partial I_\lambda(z,\vartheta,\psi)}{\rho(z)\partial z} = \alpha_\lambda(z)\left[B_\lambda(z) - I_\lambda(z,\vartheta,\psi)\right] + \sigma_\lambda(z)\left[\int_0^{2\pi} \mathrm{d}\psi' \int_0^{\pi} \gamma_\lambda(z;\vartheta,\psi;\vartheta',\psi') I_\lambda(z,\vartheta',\psi') \times \sin\vartheta'\,\mathrm{d}\vartheta' - I_\lambda(z,\vartheta,\psi)\right], \quad (5.1)$$

where ρ is the medium density; α_λ and σ_λ the spectral coefficients of absorption and scattering per unit mass of the medium (measured in $\mathrm{cm}^2\ \mathrm{g}^{-1}$, whereas the coefficients $\rho\alpha_\lambda$ and $\rho\sigma_\lambda$, calculated per unit volume, have the inverse length dimensionality); γ_λ is the spectral *scattering indicatrix* (that is, the conditional probability the scattered radiation will go in the direction **n** when the direction of incident radiation $\mathbf{n}'$ is fixed, which usually only depends on $\cos\theta = \mathbf{n}\cdot\mathbf{n}'$ of the *scattering angle* θ); B_λ is the ratio of the spectral coefficients of emission and absorption (in the approximation of local thermodynamic equilibrium, according to Kirchhoff's law, it does not depend on the nature of the absorbing medium and is a universal function of wavelength and temperature given by Planck's formula for the blackbody radiation spectrum, thus linking the fields of radiation and temperature).

If the medium contains several absorbing substances in concentrations s_k and with absorption coefficients $\alpha_{\lambda k}$ as well as scattering substances in concentrations s_l and with scattering coefficients $\sigma_{\lambda l}$ and scattering indicatrices $\gamma_{\lambda l}$, then in Eqn (5.1) we must set $\alpha_\lambda = \Sigma_k s_k \alpha_{\lambda k}$, $\sigma_\lambda = \Sigma_l s_l \sigma_{\lambda l}$, and $\sigma_\lambda\gamma_\lambda = \Sigma_l s_l \sigma_{\lambda l}\gamma_{\lambda l}$.

In the climate system one may distinguish the short-wave solar radiation and the long-wave terrestrial radiation. In the solar radiation, 99% of the energy is contained within the spectral interval $\lambda = 0.17-4$ μm (8% in the UV region 0.1–0.39 μm, 56% in the visible region 0.39–0.76 μm with the maximum in the blue light $\lambda_{\max} = 0.4738$ μm, 36% in the near IR region 0.76–4 μm, and only less than 0.4% at wavelengths $\lambda > 5$ μm). The intrinsic thermal emission of the atmosphere, the Earth's surface and the clouds falls within the range 4–100 μm (99% of the radiation energy at the temperature 300 K falls within the range 3–80 μm with the maximum at about 10 μm, and at 200 K within the range 4–120 μm with the maximum at about 15 μm; the wavelengths $\lambda < 5$ μm carry less than 0.4% of thermal radiation).

Solar and terrestrial emission spectra normalized to their respective maxima are shown in Fig. 13g. We see that these spectra practically do not overlap. The spectral range 9–12 μm is known as the 'atmospheric window'.

In the atmosphere, the short-wave radiation is scattered by microscopic inhomogeneities of air density, by suspended sub-wavelength particles [molecular or Rayleigh scattering with the indicatrix $\gamma = (3/16\pi)\times(1+\cos^2\theta)$ and scattering coefficient $\rho\sigma_\lambda = (128\pi^5/3)N\beta^2\lambda^{-4}$, where $\beta = (n^2-1)/4\pi N$ is the so-called polarizing power of the medium, n is the index of refraction, N is the number of scattering particles per unit volume] or by the larger aerosol particles and cloud particles.

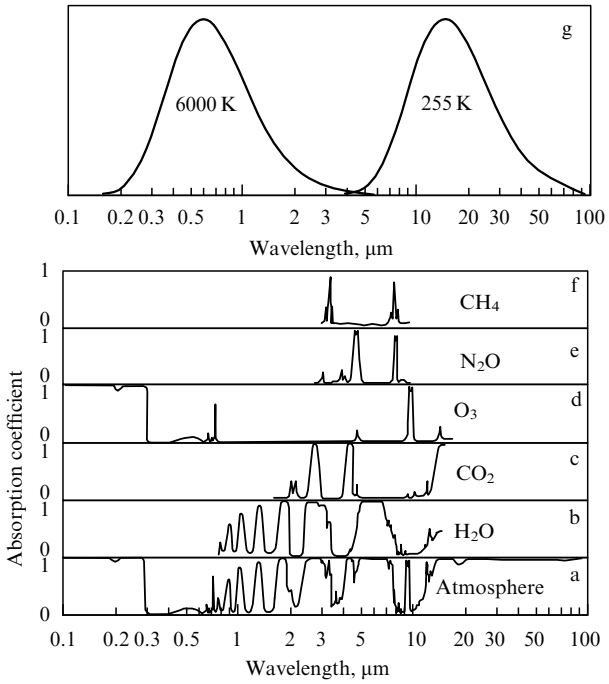

Figure 13. Absorption spectra for atmosphere (a), water vapor (b), carbon dioxide (c), ozone (d), nitrous oxide (e), methane (f), and normalized spectra of solar and terrestrial emission (g).

The Rayleigh scattering coefficient in air at normal pressure in the spectral range 0.3–1 μm is $1.5\times10^{-6}-1.1\times10^{-8}$ cm^{-1}.

Scattering indicatrices for the larger particles are highly (tenfold and more) extended in a forward direction, and the scattering coefficient in the range $\lambda = 0.6-3.8$ μm is about $\sigma_\lambda = 2500\ \mathrm{cm}^2\ \mathrm{g}^{-1}$ and decreases down to $1500\ \mathrm{cm}^2\ \mathrm{g}^{-1}$ within the range $\lambda = 2.8-3.4$ μm. The effects of aerosol particles will be given special attention in the next section.

Scattering also includes back scattering — that is, reflection of some of the solar radiation back into space. According to empirical data, the atmosphere (including clouds) reflects about 25% of the incident solar radiation q_0, and another 5% bounces from the Earth's surface. Of no less importance is the increased radiation absorption by atmospheric gases owing to the increased free path of photons (by a factor of $\overline{\cos\vartheta}$ — this quantity, known as the 'diffusion factor', can be as large as several units, for example, in clouds).

Absorption of solar radiation in the atmosphere is relatively small. Solar radiation is mainly absorbed by water vapor, ozone (and oxygen), and to a lesser extent by carbon dioxide, aerosol and cloud particles. Water vapor has weak absorption bands in the visible light (at $\lambda = 0.543-0.847$ μm) and in the near IR at $\lambda = 0.72$; 0.81 (ρ_{st}); 0.93 (Φ); 1.13 (ψ); 1.42; 1.89; 2.01–2.05 (Ω); 2.25–3.0 (χ), and 3.17 μm. Absorption by aerosol on average is comparable with that by water vapor. Carbon dioxide has five absorption bands in the near IR 1.4–4.3 μm, which are so weak as to be usually disregarded in calculations.

Ozone has two strong absorption bands in the UV region: the Hartley–Huggins band 0.22–0.29 μm (with the bulk absorption coefficient of $135\ \mathrm{cm}^{-1}$ at $\lambda = 0.255$ μm) and the band 0.31–0.36 μm, which together absorb about 4% of the solar radiation, and the weak Chappuis band in the visible

spectrum with a maximum at about $\lambda = 0.602$ μm. Molecular oxygen (O_2) absorbs ultraviolet radiation in the band 0.13 – 0.24 μm and has two narrow absorption bands in the visible spectrum at $\lambda = 0.69$ and 0.76 μm.

Altogether, the entire atmospheric depth absorbs about $a \approx 20\,\%$ of the power of the incident solar radiation. This is what we call the 'almost transparent atmosphere' — if we could make it five times as thick, without changing its chemical composition, then the absorption loss would not increase much, because the absorption spectrum still has many 'atmospheric transparency windows'.

However, the fact that ozone absorbs about 20% of the 20% solar radiation absorbed is very important, because ozone effectively stops detrimental ultraviolet radiation. This radiation is harmful for man as well — it may cause skin diseases including cancer, impairs vision (cataract), weakens the immune system. In all living organisms ultraviolet radiation may cause photolysis and denaturation of proteins (i.e. their decomposition by breaking the weak bonds between amino acids and destroying their functionality through charge reduction). Worst of all, it can affect banks of genetic information (nucleic acids) and thus interfere with the growth, division, heredity and the very existence of cells, produce mutations, and increase the probability of the emergence of new pernicious bacteria and viruses.

As early as 1879, M Cornu found that only solar radiation wavelengths longer than 0.29 μm reach the Earth's surface. R Hartley (1881) described the absorption spectrum of ozone and surmised the existence of an ozone layer in the upper atmosphere. S Chapman (1930) developed the photochemical theory of the formation and destruction of ozone in the stratosphere. At about the same time, measurements of ozone concentration in the atmosphere began, first with ground-based Dobson spectrophotometers, and later with ozone sounding balloons and satellites.

It was found that 90% of the ozone is concentrated in the stratosphere, at a height of 15 – 30 km in the mean, with a maximum partial density of the order of 5×10^{-10} g cm^{-3}. The remaining 10% is in the lower atmosphere, where ozone is produced by electrical discharges. This 'ozone shield' was formed through the gradual accumulation of free oxygen in the atmosphere about 400 – 450 million years ago, the time when living creatures moved out of the sea and onto the land.

Stratospheric ozone is produced in the chemical reactions $O_2 + h\nu \rightarrow O + O$, $O + O_2 + M \rightarrow O_3 + M(+1.09\ \text{eV})$ (where M is any third particle that carries away the released energy of 1.09 eV), and destroyed in the reactions of oxygen cycle: $O_3 + h\nu_1 \rightarrow O_2 + O$ and $O_3 + O \rightarrow 2O_2$ (where $h\nu_1$ is a quantum of UV or visible light), and in the fast catalytic reactions of chlorine cycle: $O_3 + Cl \rightarrow O_2 + ClO$, $ClO + O \rightarrow Cl + O_2$, and the similar reactions of the nitrogen and hydrogen cycles, described by the same equations with Cl replaced by NO, H, HO, and HO_2 (see, for example, the reviews [75 – 78]).

As a result, the ozone content in the column of atmosphere is rather small. It is usually expressed as the thickness of the ozone layer reduced to normal temperature and pressure, measured in millimeters (or in hundredths of millimeters known as Dobson units, 1 DU $= 2.7 \times 10^{16}$ molecules cm^{-2}). The typical ozone content is 300 DU, which corresponds to 3.2 gigatons of ozone. This value varies broadly, showing latitudinal and seasonal variations, with the minimum down to 250 DU in the tropics, and the maxima of above 460 and 400 DU, respectively, in the regions towards

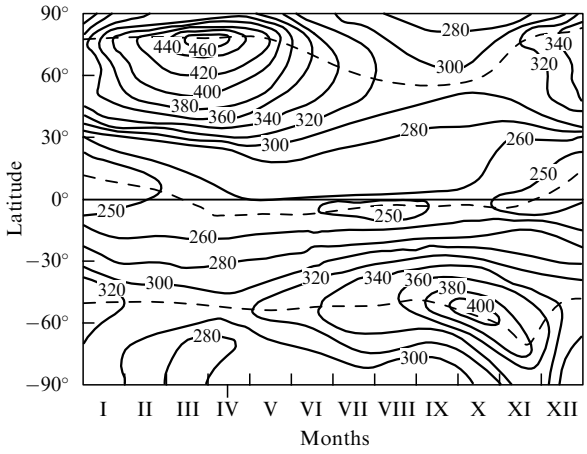

Figure 14. Isopletes of mean zonal ozone content in the atmosphere (in Dobson units) as functions of the latitude and season.

the end of polar winter: March – April in the northern hemisphere and October – November in the southern hemisphere (Fig. 14).

The ozone content also varies considerably from year to year. In Antarctic in 1985, during the 'southern spring' (in October), an 'ozone hole' was detected — a region where the ozone content was as low as 1/2 or 1/3 of the years-old norm. For example, the Holly Bay station (Graham's Land, 76° south. lat. and 27° west. long.) on 5 October 1987 registered an ozone content of 109 DU with a downward trend of 6 – 7% a year from 1958 to 1984. Later, springtime ozone holes were also found in the Arctic, and they became a recurrent phenomenon.

This ominous sign of the possible destruction of the ozone layer caused much concern within the scientific community. Currently its most probable cause is thought to be associated with the migration into the stratosphere of chlorofluorocarbons, such as $CFCl_3$ (Freon 11), CF_2Cl_2 (Freon 12), $CHFCl_2$ (Freon 21), and the like, hundreds thousands of tons of which were being produced industrially in post-war years as working fluids for refrigerators and aerosol propellants. Although it has not yet been conclusively proved that they have played a major role in ozone depletion, 31 countries have already signed the Montreal Protocol of September 1987 that limited their production (switching to other refrigerants).[2]

According to the above empirical estimates, about 55% of the incident solar radiation flux q_0 reaches the Earth's surface, 5% is then reflected back into space, and 50%, or about $q_0(1 - A - a) \approx I_0/8 \approx 170$ W m^{-2}, is absorbed by the subsurface matter of the Earth — water, soil, snow, ice and vegetation. Given that 70% of the Earth's surface is seawater, let us briefly discuss the absorption of solar radiation by the ocean.

Absorption bands of water are for the most part associated with those of water vapor, being slightly redshifted and smeared to appear as a continuous spectrum in which $\rho\alpha_\lambda$ decreases from 0.19 m^{-1} at $\lambda = 0.25$ μm to the

[2] The Montreal Protocol on substances that deplete the ozone layer, agreed upon on 16th September 1987, came into force on 1st January 1989, by when 29 countries and the EEC representing approximately 82 percent of world consumption had ratified it. Since then several other countries have joined. 172 countries are now Parties to the Protocol, of which about 130 are developing countries. (*Translator's note*.)

blue–green minimum of 0.002 m^{-1} at $\lambda = 0.46$ μm, then increases to 2.62 m^{-1} at $\lambda = 0.75$ μm, and further decreases to 2.02 m^{-1} at $\lambda = 0.8$ μm. The absorption by dissolved organic matter increases towards the shorter wavelengths (and with depth), while absorption by suspended matter shows a small maximum at $\lambda = 0.41-0.43$ μm [and in the red chlorophyll lines $\lambda = 0.67-0.68$ μm — the so-called photosynthetically active radiation (PAR)], and decreases with depth. Scattering by suspended matter is very strong and highly forward-directional.

The Earth's surface is heated by the absorbed solar radiation and then emits long-wave radiation, which in turn is scattered, reflected, absorbed and re-emitted by the atmosphere (the portion of it returned to the Earth's surface is known as the *sky counterradiation*, and the difference between radiation and counterradiation is referred to as the *effective emission* of the Earth's surface). If scattering is only accounted for through the diffusion factor $\overline{\cos\vartheta}$, then for the Earth's surface and for the upper boundary of the atmosphere from Eqn (5.1) we get the following approximate heat balance equations:

$$a_s q_0 - \left[B_s - \int_{\infty}^{0} B(z)\,\frac{\partial D(0,z)}{\partial z}\,dz\right] = q_s + q_{turb} + q_{hid} - q_P - q_{wi}\,, \tag{5.2}$$

$$q_0(1-A) = B_s D + \int_0^{\infty} B(z)\,\frac{\partial D(z,\infty)}{\partial z}\,dz\,, \tag{5.3}$$

where $a_s = 1 - A - a$; $B(z) = \sigma T^4(z)$ is the integral (with respect to wavelengths) emission function of the long-wave radiation; $D(z_1, z_2)$ is the integral function of transmission of the long-wave radiation by the atmospheric layer (z_1, z_2), and $D = D(0, \infty)$; q_s is the heat flux downward, beneath the Earth's surface; q_{turb} and q_{hid} are the turbulent fluxes of explicit and hidden heat on the Earth's surface; q_P is the heat flux carried by precipitation, and q_{wi} is the heat flux caused by freezing of water or melting of snow and ice (positive in the case of freezing). The left-hand side in Eqn (5.2) describes the radiation balance of the Earth's surface; the expression in brackets represents the effective emission from this surface.

The long-wave radiation is strongly absorbed by a number of constituents of the atmosphere, known as *greenhouse gases* (see Table 2). It is clear therefore that the transmission coefficient of the long-wave radiation for the entire atmosphere $D = D(0, \infty)$ should be small. And indeed, Golitsyn and Ginsburg [79] quote the value of $D = 0.14$ derived from empirical data of Bolle [80]. The remaining 86% of the long-wave radiation of the Earth comes not from its surface, but rather from the atmosphere.

On yearly average, the solar heat absorbed on the Earth's surface is dissipated through three mechanisms: the effective emission, and the turbulent transfer of explicit and latent heat. According to empirical estimates, the effective emission takes away one-third of this heat, whereas the other two mechanisms remove, respectively, one-ninth and five-ninths of it. Thus, the main role belongs to the turbulent transport of latent heat (together with water vapor). However, water

Table 2.

Greenhouse gas	Concentration of greenhouse gas	Contribution to greenhouse effect, deg. [24]	Coefficients of concentration increase	Increment of concentration of greenhouse gas, deg. [87]		Contribution of greenhouse gas to global warming, % [88–90]	
				At fixed cloud temperature	At fixed cloud altitude	For 1880–1980	For 1980–1990
Water vapor H_2O	2.5 g kg^{-1}	20.6	2	1.03	3.65		
Carbon dioxide CO_2	355 ppm	7.2	1.25	0.79	0.53	66	49
Ozone O_3	343 DU	2.4	0.75	−0.47	−0.34		
Nitrous oxide N_2O	0.28 ppm	1.4	2	0.68	0.44	3	6
Methane CH_4	1.3 ppm	0.8		0.28	0.20	15	18
Freon 11 $CFCl_3$	1×10^{-4} ppm	0.8	20	0.54	2.36	8	14
Freon 12 CF_2Cl_2	1×10^{-4} ppm						
Carbon tetrachloride CCl_4	1×10^{-4} ppm		2	0.02	0.01	8	13
Ammonia NH_3	6×10^{-2} ppm			0.12	0.09		
Nitric acid HNO_3	4.87×10^{-2} mm			0.08	0.06		
Ethylene C_2H_4	2×10^{-4} ppm			0.01	0.01		
Sulfur dioxide SO_2	2×10^{-3} ppm			0.03	0.02		
Methyl chloride CH_3Cl	5×10^{-4} ppm			0.02			

vapor is not only a heat carrier (to be sure, a quite efficient one thanks to the huge latent heat of water evaporation, $L \approx 2500$ J g^{-1}) — it is also a very efficient absorbent of the long-wave radiation in the atmosphere, i.e. a major greenhouse gas.

Straightforward calculation of the greenhouse effect is rather difficult owing to the complicated absorption spectra of the greenhouse gases (some of which were shown in Fig. 13). These are band spectra corresponding to the electronic, vibration and rotation energy levels of molecules. The electronic levels are characterized by quantum numbers S — the absolute values of the total spin momenta of all electrons in the molecule. Typical of the chemically stable molecules with an even number of electrons are the singlet levels with $S = 0$ and the triplet levels with $S = 1$ (levels split into $\varkappa = 2S + 1$ sublevels), while free radicals usually exhibit doublet levels with $S = 1/2$. Diatomic and linear three-atomic molecules possess an additional quantum number λ — the absolute value of projection of the total orbital momenta of all electrons onto the axis of the molecule, and the levels with $\lambda = 0, 1, 2, \ldots$ are denoted $^{\times}\Sigma$, $^{\times}\Pi$, $^{\times}\Lambda$, ...; in molecules with central symmetry we distinguish even g and odd u energy levels. Vibrational energy levels for an N-atomic molecule with f vibrational degrees of freedom ($f = 3N - 5$ for linear molecules, and $3N - 6$ for nonlinear molecules) are $\sum_{i=1}^{f} h\nu_i \times (v_i + 1/2)$, where $v_i = 0, 1, 2, \ldots$ are the vibrational quantum numbers, and ν_i are the frequencies of the normal modes (valence vibrations wherein the bond lengths vary, and deformation vibrations wherein the valence angles vary). Rotational energy levels in the simplest case of a linear molecule are $Bhj(j + 1)$, where $j = 0, 1, 2, \ldots$ is the rotational quantum number, and $B = h/8\pi^2 I$ is the rotational constant (I being the moment of inertia of the molecule with respect to its transverse axis). Finally, the intensities of absorption lines are expressed in terms of the quantum-mechanical transition probabilities (Einstein coefficients and the related matrix elements of the molecular dipole moment operator.

Observe that some contribution to the vibration – rotation bands in the molecular absorption spectra may also come (apart from intramolecular transitions) from the intermolecular transitions caused by the polarization of molecules in the course of their electrostatic and exchange interactions during collisions (known as the pressure-induced absorption). There is also continuous absorption in the wings of spectral lines in the strong vibration – rotation and rotation absorption bands.

Extensive scientific literature exists on the theoretical calculation and on the laboratory and full-scale measurements of absorption spectra of atmospheric gases (see, for example, reviews in the books by Kondrat'ev and Moskalenko [81, 24]). Among the first works of this kind was the book by Goody [82], numerical models of global atmosphere circulation with radiant heat influx by Manabe with colleagues [83, 84], and the works by Zuev [85, 86].

The principal greenhouse gas is water vapor, as was first pointed out by John Tyndall (1863). Absorption of long-wave radiation by water vapor is the highest in the vibrational band 5 – 7.5 μm with a maximum at $\lambda = 6.27$ μm, where the line-smoothed absorption coefficient is as large as 200 cm^2 g^{-1}. The spectral range 8.5 – 12 μm comprises the atmospheric transparency window where absorption by water vapor is very weak — the smoothed absorption coefficient is of the order of 0.1 cm^2 g^{-1}. In the range 12 – 100 μm, there appear the rotational bands of water vapor (supplemented in the interval 11 – 21 μm with minor absorption by the water vapor dimer).

Next in importance for terrestrial atmosphere (and about one-third as strong in magnitude of the effect) is carbon dioxide. Its greenhouse properties were first indicated by Svante Arrhenius (1896) and Thomas Chamberlain (1899). This gas has weak absorption bands near $\lambda = 4.8$ and 5.2 μm, but the strongest is the absorption in the vibrational band 12.9 – 17.1 μm centered around 15 μm, where $\alpha_\lambda = 134$ cm^2 g^{-1} and the effect of CO_2 is stronger than that of the water vapor. The observed increase in the atmospheric concentration of CO_2 (from 315 to 360 ppm from 1956 to 1997, see Fig. 15) gave strength to the notion — first voiced by D Callendar in 1938 — of the anthropogenic contribution to global warming: the release of carbon dioxide by the combustion of fossil fuels and forest fires, and unreasonably withdrew attention from the obvious positive correlation between the temperature and the content of water vapor in the atmosphere. However, this notion has not so far been conclusively confirmed or refuted by calculations of carbon dioxide content in atmosphere, ocean, and biota, and the rates of exchange between these pools.

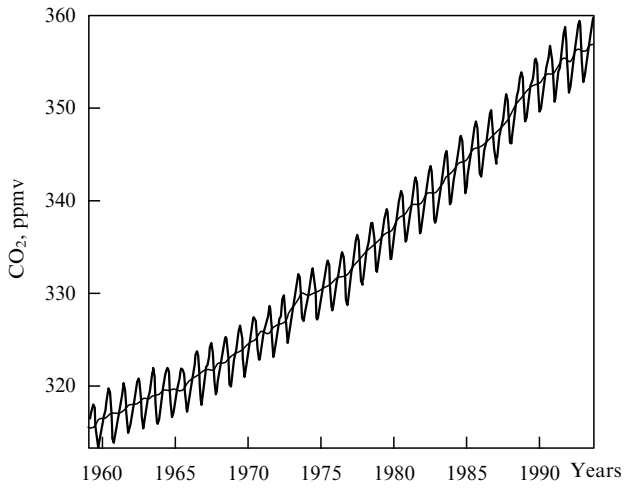

Figure 15. Variations of the volume concentration of carbon dioxide in atmosphere according to measurements at Mauna Loa, Hawaii.

At the same time, it is quite possible that warming is not the result but, conversely, the *cause* of the increase in the concentration of CO_2 in the atmosphere: heating of the ocean reduces the solubility of carbon dioxide in seawater, and the excess is released into the atmosphere. On a smaller scale this is confirmed by the seasonal oscillations of the concentration of carbon dioxide. These oscillations are very distinct in Fig. 15, where their amplitude range is as large as 5 ppm; the range increases northwards and may be as large as 15 ppm on Long Island. As this takes place, carbon dioxide is removed from the Arctic by cold ocean currents, and is released into the tropical air as the currents warm up.

The third in importance is ozone, which has strong but narrow absorption bands near 4.75 μm, and in the range of 9.35 – 11 μm within the atmospheric window centered around $\lambda = 9.569$ μm, and near 14.1 μm. Light absorption by ozone in these bands leads to heating of the stratosphere, and is vital for its very existence. Nitrous oxide has absorption bands centered at 4.54, 7.78, 8.6 and 17 μm; methane at 3.3 and 7.66 μm; Freon 11 at 9.22 and 11.82 μm; Freon 12 at 8.68,

9.13 and 10.93 μm; carbon tetrachloride at 10 and 12.99 μm, and so forth.

The second column in Table 2 gives the concentrations of greenhouse gases in ppm used in the calculations (the mean concentration of water vapor is assumed to be 2.5 g kg^{-1} — it is much greater than that of any other greenhouse gas and explains its dominant contribution to the greenhouse effect; ozone concentration is expressed in Dobson units DU; for nitric acid we give the thickness of condensed layer at standard temperature and pressure). The third column of the table gives the contribution of the substance to the greenhouse effect (in degrees centigrade) according to Kondrat'ev and Moskalenko [24]. The fourth column compiles the coefficients of concentration growth, whose effects (in degrees centigrade) are indicated in columns 5 (at constant cloud temperature) and 6 (at constant cloud altitude) according to Wong and colleagues [87]. Relative contributions (in percent) of different greenhouse gases to global warming in the periods of 1880 – 1980 and 1980 – 1990 are indicated in columns 7 and 8, respectively, according to Ramanathan and co-workers [88 – 90].

Any reliable calculations of the greenhouse effect must of course be based on complete (three-dimensional) numerical models of global atmospheric circulation with detailed inclusion of radiative and convective heat exchange, with due account taken for cloudiness and aerosols. Before that, however, it would be desirable to get an idea of the main greenhouse processes, using a simplified evaluating theory. This can be done by simplifying equations (5.2), (5.3). For this, we factor out from the integrals the mean values $B_a^{\downarrow}$ and $B_a^{\uparrow}$ of the downward and upward fluxes of long-wave radiation emitted by the atmosphere and, following Refs [79, 91] and the forerunners [92, 93], assume that they are very close to each other — that is, $B_a^{\downarrow} \approx B_a^{\uparrow} \approx \sigma T_a^4$. In a temperature-uniform atmosphere they would be exactly equal; it may be interpreted as a kind of 'convective adjustment', or correction for the 'wet convection'. Then the solution of the above equations reduces to

$$\frac{T_s}{T_{eff}} \approx \left(1 + \frac{k a_s}{1 - A}\right)^{1/4} (1 + D)^{-1/4},$$
$$\frac{T_a}{T_{eff}} \approx \left(1 - \frac{k a_s D}{1 - A}\right)^{1/4} (1 - D^2)^{-1/4}, \qquad (5.4)$$

where k is the share of the effective emission in the radiation balance of the Earth's surface. Two asymptotes can be indicated here. If all solar radiation is absorbed by the atmosphere, then $\alpha \to 1 - A$, $D \to 0$, and in this limit $T_s = T_a = T_{eff}$. If, conversely, the atmosphere is completely transparent for solar radiation, then $\alpha \to 0$, $D \to 1$, $T_s \to T_{eff}$, and $T_a \to 2^{-1/4} T_{eff}$. In between is the possibility for both the greenhouse effect $T_s > T_{eff}$ (if the atmosphere absorbs more terrestrial than solar radiation) and the anti-greenhouse effect $T_s < T_{eff}$ (if the atmosphere absorbs more solar radiation than terrestrial).

The first expression in (5.4) resolves the problem of the definition of the greenhouse effect, posed in the preceding section. It ought to be noted that in Ref. [91] the same equations (5.2), (5.3) were simplified in a somewhat different manner to give a similar approximate solution

$$\frac{T_s}{T_{eff}} \approx \left(\frac{k a_s}{1 - A}\right)^{1/4} D^{-1/4}. \qquad (5.5)$$

A more comprehensive theory must define not only the values of T_s, but also the vertical temperature profiles $T(z)$. Observe that radiative heat exchange alone (without convection) has a tendency to equalize temperatures and to form the flat profile $T(z) \equiv T_s$. Alternatively, convection alone (without radiative heat exchange and moisture condensation) tends to equalize the entropy (and its functional derivative, the so-called potential temperature $Tp^{-(\varkappa-1)/\varkappa}$) and to shape a linear temperature profile $T(z) = T_s - \gamma z$ with the adiabatic gradient $\gamma_a = g/c_p = [(\varkappa - 1)/\varkappa](g/R)$. In actuality these two extremes are not realized: the troposphere is much colder than isothermal but owing to the released heat of water vapor condensation it is warmer than adiabatic (for which with $c_p = 1003$ J g^{-1} K^{-1} we get $\gamma_a \approx 9.8$ grad km^{-1}; adiabatic stratification may occur in the atmosphere on Venus, although we do not have any indications about its stratification on the nighttime side of the planet).

All in all, however, the empirical data indicate that the troposphere is, on average, linearly stratified, although with the under-adiabatic gradient $\gamma = [(\alpha - 1)/\alpha](g/R) < \gamma_a$, where $\alpha < \varkappa$ (such stratification is hydrostatically stable), namely, we have in this region $\gamma \approx 6.5$ grad km^{-1}. Such stratification is assumed, for example, by the model of the US Committee on Extended Standard Atmosphere (COESA) of 1962, based on the following values: $p_s = 1013.25$ mbar; $T_s = 288.15$ K; $\rho_s = 1.225 \times 10^{-3}$ g cm^{-3}; $\mu = 28.9644$, and linear stratification is extended up to the altitude of 11 km. The linearity of stratification represents a very strong condition: together with the equation of hydrostatics it gives the polytrope (see Ref. [94])

$$\frac{T}{T_s} = \left(\frac{p}{p_s}\right)^{(\alpha-1)/\alpha}, \qquad (5.6)$$

which shows that $Tp^{-(\alpha-1)/\alpha}$ does not change with the altitude. This does not imply, however, that the ground-layer temperature T_s is determined by the ground pressure p_s and is proportional to $p_s^{(\alpha-1)/\alpha}$. On the contrary, such a condition would contradict the observed geographical distributions and seasonal variations of ground-layer pressures and temperatures.

6. Anti-greenhouse effect and 'nuclear winter'

Of no less importance than the greenhouse gases in the atmosphere are suspended particles — the so-called *aerosol*. This also includes the cloud particles — droplets of water and crystals of ice. Apart from their effect on radiative transfer they are the major actors in the *hydrological cycle* — the circulation of moisture, which is one of the main processes in weather and climate on the Earth and is therefore treated in a separate chapter of the physics of clouds and precipitation, which will not be given any special attention here because it is rather self-contained. Just note that many kinds of aerosol particles serve as condensation nuclei for water vapor, and when the humidity in the lower troposphere is high enough these particles are already enveloped by water.

The amount of aerosol in the atmosphere is usually not large — on the order of 60 million tons, or about 10 micrograms per square centimeter of the Earth's surface. A typical example are the sulfate particles with the radius $r \approx 0.3$ μm and the density 1.65 g cm^{-2}. To make 60 million tons it takes 3×10^{26} of such, or 50 million per square centimeter of the Earth's surface, or on average 50 particles per cubic

centimeter. If the mean lifetime of aerosol in the troposphere is the same as that of water vapor — that is, about 10 days (it is quickly washed away by rainfall), the total rate of its supply to the atmosphere is on the order of 3 gigatons per year (of which 90% come from natural sources, and only 10% are anthropogenic). Half of the natural and two-thirds of man-made aerosols result from condensation of gases.

According to Ref. [81], an aerosol is characterized by its concentration, by the distribution of particles $N(r)$ with respect to their size r (fine — from molecular size $r \sim 10^{-7}$ cm to 0.1 μm; medium — from 0.1 to 1 μm — it is this fraction that determines the optical properties of the aerosol, and particles of a size r from 1 to 10 μm are usually referred to as 'giant'), and by their contributions to the scattering σ_λ and absorption α_λ coefficients, and to the scattering indicatrix $\gamma_\lambda(\theta)$, which are calculated by the Mie theory (see, for example, Ref. [95]). *The ratio $A_\lambda = \sigma_\lambda/(\sigma_\lambda + \alpha_\lambda)$ is the albedo — that is, the probability of survival of the incident photon after single scattering*.

If an aerosol reflects some of the sunlight but lets through most of the thermal emission of the Earth, then the temperature of the aerosol-underlying atmosphere may be lower than in the absence of the aerosol. Such cooling action of the aerosol may be called the *anti-greenhouse effect*. However, the characteristics of an aerosol exhibit great variability in space and time, so under certain conditions it may even contribute to the greenhouse effect. Properties of aerosols are discussed in the reviews [15, 24, 81, 86, 96–99].

For example, according to Ref. [26], the following six kinds of natural tropospheric aerosol can be distinguished:

(1) *Marine aerosol* — particles of salt remaining after evaporation of droplets of water when sea waves break. Their rate of production is high (about 1 gigaton per year), and depends mostly on the wind velocity. These particles are rather large (their size distribution is shown in Fig. 16) and quickly settle or are washed out, being unable to pass through the 'cloud filter' at the altitudes below 3 km.

(2) *Sulfate aerosol*, already mentioned, consists of the submicron particles in the optically active range, containing ammonium sulfate $(NH_4)_2SO_4$, bisulfate NH_4HSO_4, and sulfuric acid in water solution (in the concentration of 75% in solid phase). They form in the atmosphere in the oxidation reactions of reduced sulfur compounds starting with hydrogen sulfide H_2S (see, for instance, Ref. [100]). For example, dimethylsulfide $(CH_3)_2S$ released by aquatic phytoplankton and sulfur dioxide SO_2 from various sources are oxidized (predominantly by hydroxyl OH, though SO_2 in water solution in cloud droplets is oxidized by hydrogen peroxide H_2O_2) to sulfuric acid, part of which subsequently combines with the microscopic quantities of available ammonium.

Natural production of these particles is rather high — even though it is lower than the production of marine aerosol, but the lifetime of sulfate particles in the atmosphere is longer, and they fill the entire lower troposphere up to the altitude of 5 km. In the upper troposphere, higher than 2 or 3 km above the oceans and 5 km above the continents, the sulfate particles together with mineral dust and other particles that passed through the cloud filter build up the so-called *background aerosol* (whose size distribution is also shown in Fig. 16), with a concentration of about 300 cm^{-3}.

Apparently, it is the sulfate particles that give the biggest contribution to the anti-greenhouse effect.

At the wavelength of $\lambda = 0.53$ μm, continental aerosol is characterized by values of the absorption and scattering

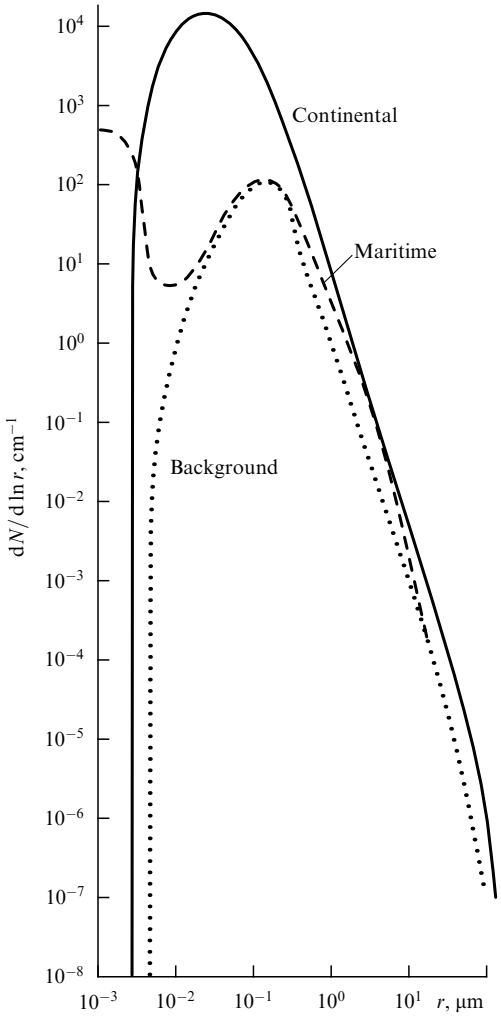

Figure 16. Typical distributions of particles with respect to size $dN/d\ln r$ (in cm^{-1}) in continental (solid line), maritime (dashed line) and background (dotted line) aerosols.

coefficients in the ranges $\rho\alpha \sim 0.007-0.07\,km^{-1}$ and $\rho\sigma \sim 0.004-0.6$ km^{-1}, the percentage of backscattering $\gamma \sim 12-28$ %, the single scattering albedo $A \sim 0.7$ in the mean, and the parameter of transition from aerosol warming to aerosol cooling $(1-A)/A\gamma \sim 0.83-5.2$ (if the albedo of the Earth's surface equals 0.2, its critical value is 2).

(3) *Desert aerosol* — mineral dust raised by sandstorms in the deserts (which occupy about 1/3 of the continents, or 8% of the Earth's surface). An example is the dust from the Sahara carried by tradewinds into the tropical Atlantic where the atmosphere often becomes so dim that the Sun at sunset becomes invisible long before its lower edge touches the horizon. Central Asian dust sometimes reaches Moscow and produces the so-called opalescent haze in the sky.

A typical desert aerosol is 75% clay minerals like montmorillonite, kaolinite, and illite, 10% calcite, and 5% each of quartz, potassium nitrate, and iron minerals (limonite, magnetite and hematite, with a small admixture of some organic compounds). The size distribution (see Fig. 16) exhibits two maxima — in the range of giant particles $r \sim 1-10$ μm, which influence the transport of thermal radiation, and in the range of $r < 1$ μm, which absorbs short-wave radiation. Their production rate is on average 0.2 Gt per year, but is highly variable. The mean concentration is

300 μg m^{-3}, and can be 3 to 10 times as large near the ground during sandstorms. For these particles, the albedo of single scattering in the visible and near infrared regions is close to one.

(4) *Biogenic aerosol* is formed from volatile organic compounds released by the plants, especially evergreens, and by certain bacteria, fungi and insects. First of all, these are *terpenes* whose molecules are built up of the so-called *isoprene groups* C_5H_8, and their companions *terpenoids* — alcohols, esters, acids, etc. One of the most common terpenes is *α-pinene* which consists of two isoprene groups (in which six of the ten carbon atoms form a benzene ring).

Terpenes are chemically very active. In particular, they bind the ozone which sometimes drifts from the stratosphere down to the Earth's surface, or is produced there by the action of UV radiation of the Sun. The resulting aerosol produces atmospheric haze. Many outdoors people will recall the bluish haze and the smell of ozone in a pine grove lit by the morning sun. Annual production of terpenes may be as high as 0.2 Gt, but their lifetime in the atmosphere is rather short, and the mean concentration of these particles is just 50 μg per cubic meter. We should also mention the sulfur-containing organic compounds called *mercaptans* which have a very pungent odor and are produced, for example, by seaweeds rotting on the shore.

(5) *Smoke aerosol* — smoke, ash, and other products of combustion of organic matter resulting from forest and steppe fires. Such fires are quite numerous on the Earth — hundreds of them are very clearly seen from satellites on the night side of the planet during hot and droughty summers. Their total production, however, is low — on average, 0.003 Gt per year, although at times it may be as high as 0.150 Gt $year^{-1}$.

(6) *Volcanic aerosol* is primarily the sulfate (and partly nitrate) aerosol formed both in the troposphere and stratosphere from volcanic gases (by oxidation of the reduced compounds of sulfur and nitrogen, including hydrogen sulfide and sulfur dioxide, which give the volcanic exhalations their infernal smell), and secondly the volcanic ash — minute particles of rock dispersed in the atmosphere during volcanic eruptions (usually the amount of ash is much greater than that of molten lava).

Contemporary Earth does not have too many volcanoes that produce such aerosol. We do not count underwater volcanoes — they contribute to the chemistry of the ocean, but not to the optics of the atmosphere. On dry land there are about 800 active volcanoes, and only 70% of them have records of eruptions. The chronology of volcanic eruptions for the past 500 years with estimates of the volume (in 10^4 m^3) of pyroclastic matter (the 'volcanic index') can be found in Refs [101–103]. The corrected excerpt from Ref. [103] for the period of 1871–1981, used in Ref. [104], contains 66 eruptions with volcanic index equal to or greater than 3. Only one-third of these have a volcanic index greater than four. It is not surprising then that the mean production rate for volcanic aerosol is not great — as low as 0.004 Gt $year^{-1}$ for volcanic ash. Part of volcanic emissions gets to the stratosphere, and the proper treatment of volcanic aerosol as a whole requires yet another type of aerosol to be distinguished — the stratospheric aerosol.

(7) *Stratospheric aerosol* (see, for example, Refs [105–108]) usually consists of sulfate particles 0.3 μm and smaller, which are droplets below 17–18 km, and solid particles at a height of 24–27 km, with the weight concentration on the order of 10^{-1} μg m^{-3}, or $10^{-1}-10^{0}$ particles per cubic centimeter, with a maximum at the altitude of 15–20 km, so that the entire layer contains in the mean 2×10^5 cm^{-2} particles whose mass is 4×10^{-2} μg cm^{-2}, or 2×10^5 t in the entire stratosphere. This aerosol is much longer-lived than the tropospheric aerosol: its mean lifetime below 20 km is about half a year, and several years above that altitude, so equilibrium is maintained by the supply of matter from the troposphere on the order of 2×10^5 t $year^{-1}$.

Normally, stratospheric aerosol constitutes about 1/300 of the global aerosol — in other words, its quantity is small, and its effect on the climate is also small. Powerful volcanic eruptions, however, may increase the amount of long-lived stratospheric aerosol by a factor of 30–100. Following such eruptions, the amount of SO_2 and aerosol in the stratosphere is reduced twofold every year, so that the norm is restored after 5 or 6 years. One must also take into account anthropogenic aerosol. Its total production is an order of magnitude lower than the production by natural sources, but the rate of production of anthropogenic sulfate aerosol and mineral dust is as high as the natural rate or even higher (see, for example, the reviews [109, 110]). For this reason, we must introduce two more types of aerosol.

(8) *Industrial sulfate aerosol* — particles formed in the atmosphere from industrial emissions of gaseous reduced sulfur compounds, mainly from sulfur dioxide SO_2. In 1977, its production was estimated at 0.13–0.20 Gt $year^{-1}$; since then it may have increased 1.5-fold; 80 or 90% comes from burning of fuels (70% from coal) to generate electricity and steam at power plants (coal contains in the mean 3.2% sulfur, fuel oil 2.8%, crude oil 0.1–5.5%, brown coal 0.2%, peat 0.1%, gasoline 0.05%; a certain amount of sulfur is found even in natural gas and firewood). The remaining 10 to 20% comes from metallurgy and production of sulfuric acid from sulfide ores (pyrites) of hydrothermal origin — extraction of copper from chalcopyrite, chalcosine, and covelline; nickel from pentlandite, zinc from sphalerite, lead from galena, mercury from cinnabar, iron from pyrite and pyrrotine, etc., which contain up to 45% of sulfur.

To give an impression of the current scale of and the prospects for world energy production, which is the main source of anthropogenic impact on the global climate, we reproduce in Fig. 17a number of diagrams from Ref. [111] (the amount of energy is expressed here in tons of so-called comparison fuel, whose heat of combustion is 7×10^6 kcal t^{-1}): curves *1* show the total energy production *E*, Gt $year^{-1}$ (12.5 Gt $year^{-1}$ in 1992); *2* — consumption per capita *e*, t $person^{-1}$ $year^{-1}$ (the current level is 2.26, i.e. one-fifth that in the US, the living minimum is 1.35 and is not reached in many countries); *3*, *4*, *5*, *6* — the structure of consumption of commercial energy in Gt $year^{-1}$ (solid fuel, liquid fuel, gas, other sources); *7*, *8*, *9* — cumulative energy consumption in Gt starting from 1990 (coal, oil, gas — is the expedience of the development of coal mining industry very clear); *10* — emission of carbon dioxide CO_2 (in Gt of carbon per year), and *11* — concentration of CO_2 in atmosphere in ppm. The forecasts in Fig. 17, however, are based on historical extrapolation — the continuing low level of energy consumption for the majority of the world population, which is in line with the strategy of the 'golden billion' and ensures social instability. Therefore, it does not seem plausible (much like a laminar flow of fluid at very large Reynolds numbers).

Sulfate aerosol also leads to acid rainfall, sulfuric and partly nitric ('acid rain'). This phenomenon was first detected

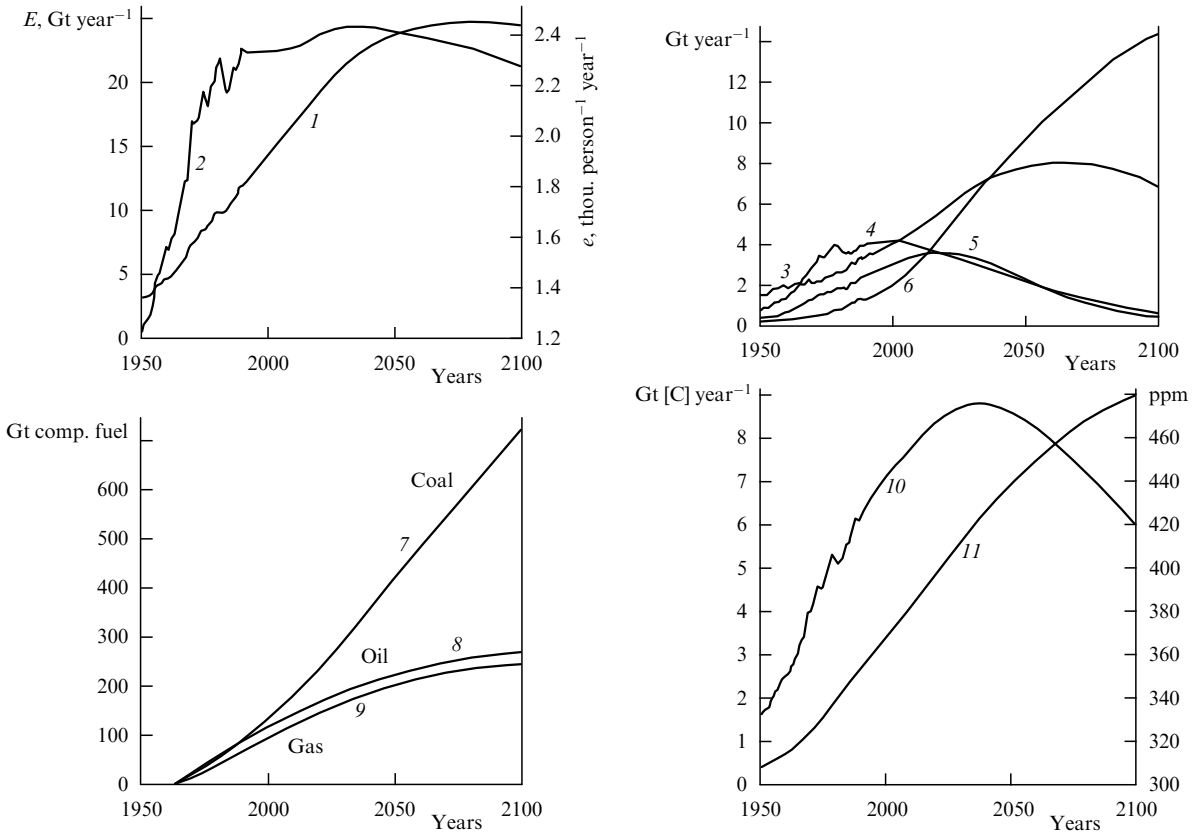

Figure 17. Current state and forecast for the next century of the development of the world power industry [111]: *1* — total energy production; *2* — consumption per capita; *3*, *4*, *5*, *6* — structure of energy consumption (solid fuel, liquid fuel, gas, other sources); cumulative energy consumption starting from 1990 (*7*, *8*, *9* — coal, oil, gas); *10* — emission of carbon dioxide; *11* — atmospheric concentration of carbon dioxide.

in 1962 in the water of a mountain lake in Sweden, and later became quite common in the north-western US and in Western Europe. The acidity of a solution is measured by the so-called pH value, numerically equal to less than 7 for acid solutions and decreasing with increasing acidity. The pH value of atmospheric precipitation was 5.2 to 5.6 in the pre-industrial epoch, 5.7 in pure natural water. Today in the north-western US, the rainfall has pH = 4.2 (sometimes 3.6 – 2.6 in the lower cloud layer); in Western Europe pH = 4 – 3.3. In the Los Angeles smog, the recorded value of pH was as low as 2 (the acidity of lemon juice), and the pH value reconstructed for the disastrous London smog of 1952 was 1.6.

Acid rains, especially combined with the increased concentration of sulfur dioxide, suppress vegetation: the stomas of leaves and coniferous needles open up, evaporation increases, and the plant withers ('physiological drought'). Acid rain has already destroyed vast areas of coniferous forests (incidentally, lichens are 100 times more sensitive, which makes them good indicators of sulfuric pollution). Increased acidity also oppresses fish — in the rivers of southern Norway, famous for their salmon in the beginning of this century, not a single salmon was caught in 1970. Finally, sulfuric pollution harms buildings and monuments of limestone and marble. In Florence they have had to move the famous marble statue of David by Michelangelo Buonarroti from an open space on the square into a shelter; acid rain is eating away the splendid Parthenon on the Acropolis at Athens, the Colosseum and Arch of Titus in Rome, Saint Mark's Church in Venice, Cleopatra's obelisk in London, the gothic Cathedral of Cologne, etc.

(9) *Industrial dust* is produced primarily by the mining industry, both by open quarries where ore or coal are loaded into trucks by huge excavators, and by coal and ore mines which accumulate huge waste heaps. Another significant contribution results from cement plants, which have to crush at least three tons of rock for every ton of cement — and the world's annual production of cement is half a billion metric tons. These two industries, together with the emissions of the metals industry, produce as much as 0.045 Gt year^{-1} of industrial dust, smoke and ash.

According to findings reported in Ref. [100], sulfate aerosol scatters about 3% of direct solar radiation, of which 15 – 20% returns back into space, or 0.5% of the total; with a mean cloudiness of 0.5 this value goes down to 0.2 or 0.3% of the solar radiation that reaches the surface of the Earth. The power of the latter amounts to about 200 W m^{-2}, and so the anti-greenhouse effect is from 0.4 to 0.6 W m^{-2}, and about 1 W m^{-2} in the northern hemisphere with its extensive industry. This value is comparable with the greenhouse effect of 1.5 W m^{-2} from the anthropogenic carbon dioxide (but less than 2 or 2.5 W m^{-2} from all anthropogenic greenhouse gases). More detailed calculations gave a value for the anti- greenhouse effecting over 2 W m^{-2} for eastern US, and up to 4 W m^{-2} for Europe and the Middle East; the average for the northern hemisphere is 1.1 W m^{-2} (observe that the effects of aerosol and greenhouse gases do not cancel out, because they are separated in space and time: the former is the strongest in the northern hemisphere in summer, and works only in the daytime, while the latter is distributed more evenly).

The resulting estimates of the anti-greenhouse effects of an aerosol are not great. It would be wrong, however, to write them off as negligible, because one must take into account the effects of huge (although rare) volcanic eruptions. They strike the imagination with their overpowering strength. Around 1250 BC the eruption of the Santorini volcano destroyed the great palace of Knossos, the center of the Minoan civilization on the north coast of Crete, leaving behind the legend of Atlantis that sunk beneath the sea. In 79 BC the eruption of Vesuvius on the Bay of Naples buried the cities of Herculaneum and Pompeii under tons of lava, mud, and ashes. In August 1883, the eruption of Krakatau (Indonesia) shot about 20 km^3 of pyroclastics up to a height of 80 km; ash from the eruption colored daybreaks around the world for several years (a similar, but even more powerful, eruption that had taken place in April 1815 at Mt. Tambora on the Indonesian island of Sumbawa and threw up as much as 150 km^3 of debris into the atmosphere did not attract appropriate notice, probably because of the low degree of informatization of society). On 8 May 1902, the eruption of Mt. Pelee on Martinique burned the town of Saint Pierre with 28,000 people. The eruption of Katmai volcano in Alaska in June 1912 was comparable with the Krakatau explosion.

Impressed by these phenomena, W Humphries (1913, 1929) put forward the hypotheses that powerful volcanic eruptions lead to global cold snaps, and that the glacial periods of the last million years of the Earth's history were caused by increased global volcanic activity (the latter conjecture does not hold water, because the intensity of global volcanic activity is governed by the tectonic processes, whose characteristic times are two or three orders of magnitude greater than the duration of glacial periods). The linkage between volcanism and climate even now is discussed in special books — see, for example, Refs [112, 107].

In the second half of the 20th century, special aerosol measurements were made after a number of strong eruptions (Agung, 1963; Fuego, 1974; Mt. St. Helens, 1980; El Chichon, 1982, etc.), and the volcanic indices were correlated to the zonally or globally averaged air temperatures (see, for example, Refs [113, 114]). The results, however, were not consistent — probably because of the dubious methods of averaging — and it was only after the Pinatubo (Philippines) eruption (1991) that Hansen with colleagues [9] were able to reliably detect a global fall of temperature, which allowed them to call the period of 1992–1995 'the return to the pre-Pinatubo level'.

It seems that today we may state with confidence that *powerful volcanic eruptions make a considerable contribution to the 'vibrations of climate'* mentioned in the Introduction and illustrated in Fig. 2.

However, even after the strongest eruptions the unclouded atmosphere remains relatively transparent: we see the stars, and not only the outlines of continents, but many small details (sometimes a few meters across) are visible from satellites. The terrestrial atmosphere could have been made opaque only by a catastrophe of cosmic scale.

In the Solar system only Venus, Uranus and Titan have turbid atmospheres. On Venus it is a thick and opaque layer of dilute fog at an altitude of 48–67 kilometers, consisting of micron-sized droplets of water solution of sulfuric acid, resembling the stratospheric sulfate aerosol (but somewhat larger). The above-cloud layer of the hydrogen–helium atmosphere of Uranus (with 2% methane) contains a semitransparent mist of submicron particles, through which are visible the bright zones and dark cloud belts at levels with pressure of 0.9 to 1.3 atm (from tiny crystals of methane ice), typical of the zonal circulation on rapidly rotating planets. The fourteenth satellite of Saturn, the giant Titan (bigger than Mercury) has an opaque atmosphere of nitrogen with 6% methane and small additions; radio sounding detected a three-layer haze of submicron particles here; the pressure and the temperature at its bottom were found to be 1.6 atm and about 95 K — this atmosphere is both very thick and very cool.

The thin atmosphere of Mars is both usually transparent, and small clouds are sometimes seen — yellow (dust) and blue (water). As early as 1909, Antoniadi suggested that the yellow clouds should develop more actively when Mars is near its perihelion (the Martian year is 1.88 y of ours). This was confirmed by later observations [115, 116]. The inclination of the axis of rotation relative to the plane of the orbit in the modern astronomical epoch is such that near the perihelion (when the insolation is 20% above average) the summer comes in its southern hemisphere. The southern ice cap quickly melts, and the atmosphere rapidly flows to the wintertime northern ice cap, causing strong winds and raising dust from the surface. Sometime this leads to global sandstorms (they are not strictly periodical, but rather cyclic — perhaps much more so than is observed on the Earth with the monsoons of Southern Asia). This process is especially well seen from the Earth at the times of the so-called favorable oppositions, when the Earth is on the same side of the Sun as Mars, the distance between the planets is at its smallest, and the entire disk of Mars is illuminated by the Sun. Such geometry occurs every 15 or 17 years.

During the favorable opposition in November 1971, Mars was approached by space probes Mariner 9 (USA), and later by Mars 2 and 3 (USSR); the pictures they radioed showed that the planet was shrouded in a global dust storm, through which only the top calderas of the giant shield volcanoes in the Tarsis region with heights higher than 20 km were visible. This dust storm lasted for more than four months. Later measurements by landing modules revealed that the surface temperature below the storm falls by 10–15 degrees, and the vertical air temperature profile flattens out.

The global dust storm on Mars may serve as a model for certain aspects of terrestrial cataclysms. The development of such storms, starting with the raising of dust into the atmosphere (the so-called saltation, and the convective whirlwinds — the 'dust devils', so vividly pictured by Alexander Blok in his drama 'King on the Town Square'[3]) all the way to self-organization processes (including anti-greenhouse cold snap beneath the dust clouds, circulation between their cold cores and warm peripheries, generation of 'thermal wind') was analyzed in the works of Golitsyn [117, 64, 79] and other authors [118–133].

In Ref. [79], the temperatures during the dust storm were calculated from the approximate formulas (5.4), in which they set $k = 1$, and the unperturbed values $a_s = 0.76$ and $D = 0.76$ were multiplied by $\exp(-r_s\Delta\tau_s)$ and $\exp(-r\Delta\tau)$, where $\Delta\tau_s$ and $\Delta\tau$ are the increments in the optical thicknesses for solar and thermal radiation, and r_s and $r = 1.66$ are the diffusion factors, whereas $\tau_s \approx 4\tau$. The resulting T_a and T_s as functions of $\Delta\tau$ are shown in Fig. 18a, from which we see that at

[3] Alexander Blok (1880–1921), Russian poet, metaphorically depicted dust devils as 'little red rumors' that ran over town and incited civil unrest. (*Translator's note*.)

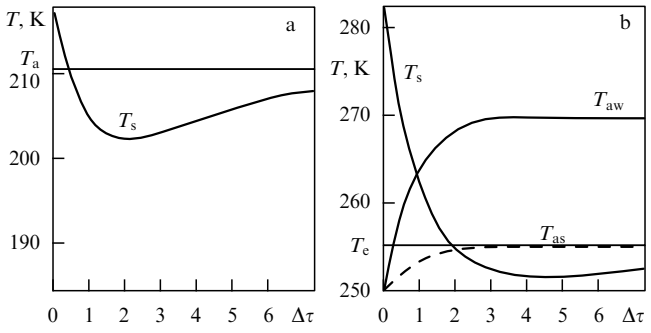

Figure 18. (a) Values of T_s and T_a as functions of the optical thickness $\Delta\tau$ of the dust layer for thermal radiation during a Martian dust storm [79]. (b) Same after nuclear war [143]: T_{as} — temperature of atmosphere above land; T_{aw} — temperature of atmosphere above ocean.

$\Delta\tau > 0.2$ there is the anti-greenhouse effect.

A catastrophic dimming of the Earth's atmosphere, mentioned earlier, could result from a nuclear war. We know that the governments of the two superpowers, afflicted by a ruinous deficiency of scientific reasoning, have jointly hoarded 20 billion tons of nuclear explosives in TNT equivalent — an amount sufficient for destroying all life on Earth many times. But perhaps not everybody knows that even without the radioactivity the dimming of the atmosphere caused by thousands of megaton explosions may lead to catastrophic cooling (possibly irreversible) because of the anti-greenhouse effect — the so-called 'nuclear winter'.

The first publication specially devoted to this topic was apparently the paper by Crutzen and Birks [134] of 1982, followed by the series of works by Golitsyn with colleagues [79, 135–144], Moiseev's group [145–156], other Russian [22, 26, 157–161] and foreign [162–168] authors.

Some remarks are due in connection with these publications. After the bankruptcy of the policy of nonproliferation of nuclear weapons (characteristic of the contemporary society of the 'golden billion'), the over-conservative treatment of the possible climate catastrophe by five American experts TTAP [162] may be dangerous. What seem to be more realistic estimates were made in Refs [79, 143], where the approximate equations (5.4) were derived and used with $\tau_s \approx 10\tau$, corresponding to the smoke aerosol of nuclear winter. The anti-greenhouse effect of such aerosol is greater than 30 °C, which completely annihilates the effects of greenhouse gases.

Calculations of the nuclear winter in Refs [147, 163] were based on specially constructed numerical models of the climate system. The results of such calculations, summarized in Ref. [149], include the conclusion that the state of 'white Earth' brought about by nuclear winter is irreversible, owing to the increase of planetary albedo and the disappearance of the greenhouse effect of water vapor because of its freezing. It should be admitted, however, that numerical models are not capable of giving a formal proof of the stability of any given state of the simulated system. Finally, we would like to mention a comprehensive two-volume collection of papers published by the International Committee for the environment [167], and a popular book by Lydia Dotto [168].

A natural analogue of nuclear winter could be brought about by the impact of a very large meteorite — say, 10 kilometers across. Alvarez with colleagues [169] suggested that such an impact could have taken place 65 million years ago, marking the boundary between the Mesozoic and Cenozoic eras and, in particular, leading to the extinction of the dinosaurs: on some geological cross-sections they found a thin clay layer corresponding to that age, rich in iridium. Some evidence in favor of the Alvarez hypothesis was collected in Ref. [143]. In our book [170], however, we advocate the opposite view of the continuity of life, which includes the continuity of the formation, flourishing and extinction of different forms of living organisms. In any case, the hypothesis of Alvarez will be eventually confirmed or refuted not by climatologists, but by geologists and paleontologists.

References

1. Manley G *Quart. J. R. Met. Soc.* **79** 242 (1953)
2. Manley G *Quart. J. R. Met. Soc.* **100** 389 (1974)
3. Bradley R S, Jones P D *The Holocene* **3** 387 (1993)
4. Monin A S, Shishkov Yu A *Istoriya Klimata* (Climate History) (Leningrad: Gidrometizdat, 1979)
5. *Polnoe Sobranie Russkikh Letopiseĭ* (Complete Set of Russian Chronicles) Vol. 14, Pt. 1 (St. Petersburg, 1910) p. 55
6. Monin A S, Shishkov Yu A *Nauki o Zemle* Vyp. 7 (Earth Sciences) (Moscow: Znanie, 1990)
7. Hansen J, Lebedeff S *J. Geophys. Res.* **92** 13.345–13.372 (1987)
8. Hansen J, Lebedeff S *Geophys. Res. Lett.* **15** 323 (1988)
9. Hansen J, Ruedy R, Sato M, Reynolds R *Geophys. Res. Lett.* **23** 1665 (1996)
10. Jones P D, Wigley T M L, Gregory J M "Trend 93" 975 (Oak Ridge, 1994)
11. Lorenz E N *J. Atm. Sci.* **20** (5) 448 (1963)
12. Lorenz E N *Met. Monogr.* **30** 1 (1968)
13. Lorenz E N *J. Appl. Met.* **9** 325 (1970)
14. Monin A S *Vrashchenie Zemli i Klimat* (Earth's Rotation and Climate) (Leningrad: Gidrometizdat, 1972) [Translated into English (Delhi: Radok-Radhakrishna, 1974)
15. Monin A S *Vvedenie v Teoriyu Klimata* (An Introduction to the Climate Theory) (Leningrad: Gidrometizdat, 1982) [Translated into English (Dordrecht: D. Reidel Publ. Co., 1986)]
16. Monin A S *Dokl. Ross. Akad. Nauk* **328** 395 (1993)
17. *The Physical Basis of Climate and Climate Modelling* Ser. 16 (GARP Publ., 1975)
18. Monin A S, Gavrilin B L *Gidrodinamicheskiĭ Prognoz Pogody* (Hydrodynamic Weather Forecast) (Leningrad: Gidrometizdat, 1977) p. 56
19. Kitting M *Programme of Action. Publication of the Center* "For Our Common Future" (Geneva, 1993)
20. Kutzbach J E, Bryson R A *J. Atm. Sci.* **31** 1958 (1974)
21. Fedorov E E, Baranov A I *Klimat Ravniny ETS v Pogodakh* (Climate of the Plain of the European Territory of the USSR in Weathers) (Moscow–Leningrad, 1949)
22. Kondrat'ev K Ya *Itogi Nauki i Tekhniki, Ser. Meteorol., Klimatol.* Vol. 6 (1981), Vol. 8 (1982), Vol. 16 (1986)
23. Kondrat'ev K Ya *Sputnikovaya Klimatologiya* (Satellite Climatology) (Moscow: Gidrometeoizdat, 1983)
24. Kondrat'ev K Ya, Moskalenko N I *Itogi Nauki i Tekhniki, Ser. Meteorol., Klimatol.* Vol. 12 (1984)
25. Kondrat'ev K Ya, Prokof'ev M A *Itogi Nauki i Tekhniki, Ser. Meteorol., Klimatol.* Vol. 11 (1983)
26. Kondrat'ev K Ya *Global'nyĭ Klimat i Ego Izmeneniya* (Global Climate and Its Changes) (Leningrad: Nauka, 1987)
27. Willson R C, Gulkis S et al. *Science* **211** 700 (1981)
28. Wood R M *Nature* (London) **255** 312 (1975)
29. Prokudina V S *Soobshcheniya GAISh* 44 (1978)
30. Avsyuk Yu N *Prilivnye Sily i Prirodnye Protsessy* (Tidal Forces and Natural Processes) (Moscow: OIFZ RAN, 1996)
31. Landsberg H E, Mitchell J M, Gruntcher H L *Monthly Weather Rev.* **87** (8) (1959)
32. Brier G W *Ann. N. Y. Acad. Sci.* **95** art. 1 (1961)
33. Kolesnikova V N, Monin A S *Meteorol. Issled.* **16** 30 (1968)
34. Vulis I L, Monin A S *Dokl. Akad. Nauk SSSR* **197** (2) 328 (1971)

35. Vulis I L, Monin A S *Tellus* **13** (4 – 5) 337 (1971)
36. Monin A S *Rannyaya Geologicheskaya Istoriya Zemli* (Early Geological History of the Earth) (Moscow: Nedra, 1987)
37. McDonald J F *Rev. Geophys.* **2** (4) 467 (1964)
38. Milankovich M *Glas. Srpske K. Akad. Belgrade* **91** 101 (1913)
39. Milankovich M *Bull. Trav. Akad. Sci. Zagreb* (1915)
40. Milankovich M *Theorie math. des phenomenes therm. produits par la radiation solaire, Ac. Yougoslave Sci. Arts Zagreb* (1920)
41. Milankovich M *Bull. Ac. R. Serbe Sci. Math. nat. Belgrade A* **4** (1938)
42. Milankovich M *Handb. Geophys. Berlin* **9** 593 (1938)
43. Milankovitch M *Mathematische Klimalehre und Astronomische Theorie der Klimaschwankungen* (Mathematical Climatology and the Astronomical Theory of Climate Oscillations) (Berlin, 1930) [Translated into Russian (Moscow – Leningrad: GONTI, 1939)]
44. Milankovich M *Canon der Erdbestrahlung und seine Anwend. auf das Eiszeitenproblem Belgrade* (1941)
45. Vorob'ev V I, Monin A S *Fiz. Atm. Okeana* **11** (9) 383 (1975)
46. Vulis I L, Monin A S *Dokl. Akad. Nauk SSSR* **242** (5) 1034 (1978)
47. Vulis I L, Monin A S *Fiz. Atm. Okeana* **15** (1) 3 (1979)
48. Monin A S *Dokl. Akad. Nauk SSSR* **249** (2) 319 (1979) [*Sov. Phys. Dokl.* **24** 872 (1979)]
49. Sharaf Sh G, Budnikova N A *Bull. ITA* **11** (4) 231 (1967)
50. Sharaf Sh G, Budnikova N A *Dokl. Akad. Nauk SSSR* **182** (2) 291 (1968)
51. Sharaf Sh G, Budnikova N A *Bull. ITA* **14** 48 (1969)
52. Bretagnon P *Astron. Astrophys.* **30** 141 (1974)
53. Berger A *Celes. Mech.* **15** (1) (1977)
54. Woldstedt P *Das Eiszeitalter Stuttgart* **1** (1954)
55. Murray B, Malin M *Science* **179** 997 (1973)
56. Murray B, Ward W, Young S *Science* **180** 638 (1973)
57. Ward W *Science* **181** 260 (1973)
58. Ward W *J. Geophys. Res.* **79** 3375 (1974)
59. Sharaf Sh G, Budnikova N A *Dokl. Akad. Nauk SSSR* **221** (1) 64 (1975) [*Sov. Phys. Dokl.* **20** 155 (1975)]
60. Sharaf Sh G, Budnikova N A *Trudy ITA* **16** (1977)
61. Golitsyn G S *Dokl. Akad. Nauk SSSR* **190** (2) 326 (1970)
62. Golitsyn G S *Icarus* **13** (1) 1 (1970)
63. Golitsyn G S *Fiz. Atm. Okeana* **7** (9) 974 (1971)
64. Golitsyn G S *Vvedenie v Dinamiku Planetnykh Atmosfer* (Introduction to the Dynamics of Planetary Atmospheres) (Leningrad: Gidrometizdat, 1973)
65. Zilitinkevich S S, Monin A S *Fiz. Atm. Okeana* **9** (8) 871 (1973)
66. Zilitinkevich S S, Monin A S *Dokl. Akad. Nauk SSSR* **226** (6) 1311 (1976)
67. Zilitinkevich S S, Monin A S *Global'noe Vzaimodeĭstvie Atmosfery i Okeana* (Global Interaction between Atmosphere and Ocean) (Leningrad: Gidrometizdat, 1977) p. 23
68. Monin A S, Zilitinkevich S S *J. Atm. Sci.* **34** 1214 (1977)
69. Kuznetsov E S *Izv. Akad. Nauk SSSR Ser. Geogr. Geofiz.* **5** (1943)
70. Kuznetsov E S *Izv. Akad. Nauk SSSR Ser. Geogr. Geofiz.* **4** (1954)
71. Kondrat'ev K Ya *Luchistaya Energiya Solntsa* (Radiant Energy of the Sun) (Leningrad: Gidrometizdat, 1954)
72. Kondratyev K Ya *Radiation in the Atmosphere* (New York: Academic Press, 1969)
73. Kondratyev K Ya *Radiation Processes in the Atmosphere. WMO Monograph* **39** (1972)
74. Sobolev V V *Rasseyanie Sveta v Atmosferakh Planet* (Light Scattering in Planetary Atmospheres) (Moscow: Nauka, 1972) [Translated into English (Oxford: Pergamon Press, 1975)]
75. Grutzen P J *Can. J. Chem.* **52** 1569 (1974)
76. Stolarski R S, Cicerone R J *Can. J. Chem.* **52** 1582 (1974)
77. Nicolet M *Can. J. Chem.* **52** 1381 (1974)
78. McConnell J C *Can. J. Chem.* **52** 1625 (1974)
79. Golitsyn G S, Ginsburg A S *Tellus* **378** 173 (1985)
80. Bolle H J, in *Handb. of Environ. Chem.* Vol. 1 (Berlin: Springer-Verlag, 1982) p. 131
81. Kondrat'ev K Ya, Moskalenko N I *Teplovoe Izluchenie Planet* (Thermal Radiation of Planets) (Leningrad: Gidrometizdat, 1977)
82. Goody R M *Atmospheric Radiation* (Oxford: Oxford University Press, 1964)
83. Manabe S, Strickler R *J. Atm. Sci.* **21** (4) 361 (1964)
84. Manabe S, Wetherald R T *J. Atm. Sci.* **24** (2) 211 (1969); **32** (1) 3 (1975); **37** (1) 99 (1980)
85. Zuev V E et al. *Opt. Spektrosk.* **25** (1) 36 (1968)
86. Zuev V E *Rasprostranenie Vidimykh i Infrakrasnykh Voln v Atmosfere* (Propagation of Visible and Infrared Radiation in the Atmosphere) (Moscow: Sovetskoe Radio, 1970) [Translated into English (New York: Wiley, 1974)]
87. Wong W S, Yung J L, Lacis A A et al. *Science* **194** 685 (1976)
88. Ramanathan V, Coakley J A *Rev. Geophys. Space Phys.* **6** 465 (1978)
89. Ramanathan V, Lian M S, Cess R D *J. Geophys. Res.* **84** 4949 (1979)
90. Ramanathan V, Cicerone R S, Singh H B, Kiehl J T *J. Geophys. Res. D* **90** 5547 (1985)
91. Ginzburg A S *Izv. Akad. Nauk SSSR Ser. Fiz. Atm. Okeana* **18** (12) 1262 (1982)
92. Feĭgel'son E M *Luchistyĭ Teploobmen i Oblaka* (Radiative Heat Exchange and Clouds) (Leningrad: Gidrometeoizdat, 1970) [Translated into English: *Radiant Heat Transfer in a Cloudy Atmosphere* (Jerusalem: Israel Program for Scientific Translations, 1973)]
93. Ginzburg A S, Feĭgel'son E M *Izv. Akad. Nauk SSSR Ser. Fiz. Atm. Okeana* **7** (4) 377 (1971)
94. Monin A S *Izv. Akad. Nauk SSSR Ser. Geofiz.* **4** 761 (1952)
95. Deirmendjian D *Electromagnetic Scattering on Spherical Polydispersions* (New York: Wiley, 1969) [Translated into Russian (Moscow: Mir, 1971)]
96. Goody R M *Atmospheric Radiation* (Oxford: Clarendon Press, 1964)
97. Kondrat'ev K Ya (Ed.) *Vliyanie Aerozolya na Perenos Izlucheniya: Vozmozhnye Klimaticheskie Posledstviya* (Aerosol Effects on Radiation Transfer: Possible Climatic Consequences) (Leningrad: Izd. LGU, 1973)
98. Kondrat'ev K Ya, Moskalenko N I, Pozdnyakov A N *Atmosfernyĭ Aerozol'* (Atmospheric Aerosol) (Leningrad: Izd. LGU, 1983)
99. Kondrat'ev K Ya *Itogi Nauki i Tekhniki Ser. Meteorol., Klimatol.* **10** (1983)
100. Charlson R J, Wigley T M L *Sci. Am.* **270** (2) 48 (1994)
101. Simkin T et al. *Volcanoes of the World, Smithsonian Inst.* (1981, suppl. 1985)
102. Simkin T et al. *Global Volcanism 1975 – 1985* (Washington: Amer. Geophys. Union, 1989)
103. Newhall C G, Self S *J. Geophys. Res.* **87** 1231 (1982)
104. Handler P, O'Neill B *J. Geophys. Res.* **92** 14621 (1987)
105. Lenoble J et al. *J. Atm. Sci.* **39** 2565 (1982)
106. Deschamps P J et al. *Adv. Space Res.* **2** (5) 171 (1985)
107. Khmelevtsov S S (Ed.) *Vulkany, Stratosfernyĭ Aerosol' i Klimat Zemli* (Volcanoes, Stratospheric Aerosol, and Climate of the Earth) (Leningrad: Gidrometeoizdat, 1986)
108. Roser J M, Hoffman D J *Appl. Opt.* **25** (3) 410 (1996)
109. Monin A S, Shishkov Yu A *Nauki o Zemle* Vyp. 6 (Earth Sciences) (Moscow: Znanie, 1991)
110. Monin A S *Ekologiya dlya Vsekh* (Ecology for Everyone) (Moscow–Perm', 1995)
111. Snytin S Yu, Klimenko V V, Fedorov M V *Dokl. Ross. Akad. Nauk* **336** (4) 476 (1994) [*Phys. Dokl.* **39** 457 (1994)]
112. Kondrat'ev K Ya *Itogi Nauki i Tekhniki. Ser. Meteorol., Klimatol.* **14** (1985)
113. Angell J K, Korshover J *Month. Weather Rev.* **112** 1457 (1984); *J. Clim. Appl. Meteorol.* **24** 937 (1985)
114. Schönwiese C D *Atmosfera* **1** 141 (1988)
115. Gifford F A *Month. Weather Rev.* **92** (18) 135 (1964)
116. Glasstone S *The Book of Mars. NASA Publ.* (1968)
117. Golitsyn G S *Icarus* **18** (2) 113 (1973)
118. Gierasch P, Goody R *Planet. Space Sci.* **16** 615 (1968)
119. Leovy C B, Mintz Y *J. Atm. Sci.* **26** 1167 (1969)
120. Sagan C, Pollack J B *Nature* (London) **223** 791 (1969)
121. Sagan C, Veverka J, Gierasch P *Icarus* **15** (2) 253 (1971)
122. Gierasch P, Goody R *J. Atm. Sci.* **29** (2) 400 (1972)
123. Caper C F, Martin L J *Sky a. Telescope* **49** (5) 276 (1972)
124. Leovy C B et al. *Icarus* **17** (2) 373 (1972)
125. Morozhenko A V *Astronom. Tsirkulyar* **683** 1 (1972)
126. Steinbacher R H et al. *Science* **175** (21) 293 (1972)
127. Hess S L *Planet. Space Sci.* **21** (1973)
128. Kondrat'ev K Ya, Bunakova A M *Meteorologiya Marsa* (Meteorology of the Mars) (Leningrad, 1973)

129. Kondrat'ev K Ya et al. *Dokl. Akad. Nauk SSSR* **211** (4) 801 (1973)
130. Gierasch P *Rev. Geophys. Space Phys.* **12** 730 (1974)
131. Pollack J B et al. *J. Geophys. Res.* **84** 2929 (1979)
132. Ryan J A, Henry R M *J. Geophys. Res.* **84** 2821 (1979)
133. Zurek R W *Icarus* **50** 288 (1982)
134. Crutzen P J, Birks J W *Ambio* **11** 115 (1982)
135. Obukhov A M, Golitsyn G S *Zemlya i Vselennaya* (6) 5 (1983)
136. Golitsyn G S *Vestn. Akad. Nauk SSSR* **9** 57 (1983)
137. Golitsyn G S, Ginzburg A S, Preprint IFA AN SSSR (Moscow: IFA Publ., 1983)
138. Obukhov A M, Golitsyn G S, in *Mir i Razoruzhenie* (Peace and Disarmament) (Ed. P N Fedoseev) (Moscow: Nauka, 1984)
139. Golitsyn G S *Priroda* (6) 22 (1985)
140. Budyko M I, Golitsyn G S, Izrael' Yu A *Global'nye Klimaticheskie Katastrofy* (Global Climatic Catastrophes) (Leningrad: Gidrometeoizdat, 1985) [Translated into English (Berlin: Springer-Verlag, 1988)]
141. Ginsburg A S, Golitsyn G S, Vasiliev A A *SIPRI Year Book* 107 (1985)
142. Golitsyn G S, Phillips N A *Rep. WMO* (Geneva, 1985); *World Climate Pap.* **113** 17 (1986)
143. Golitsyn G S, Ginzburg A S, in *Klimaticheskie i Biologicheskie Posledstviya Atomnoĭ Voĭny* (Climatic and Biological Effect of Nuclear War) (Moscow, 1986) p. 100
144. Turco R P, Golitsyn G S *Environment* **30** (5) 8 (1988)
145. Aleksandrov V V et al. *Izv. Akad. Nauk SSSR Ser. Fiz. Atm. Okeana* **19** 451 (1983)
146. Alexandrov V V, Stenchikov G L *Proc. Appl. Math. Comput. Center AS USSR* (1983)
147. Aleksandrov V V, Stenchikov G L *Zh. Vychisl. Mat. Mat. Fiz.* **14** 140 (1984)
148. Thompson S L et al. *Ambio* **13** 236 (1984)
149. Moiseev N N, Aleksandrov V V, Tarko A M *Chelovek i Biosfera* (Man and Biosphere) (Moscow: Nauka, 1985)
150. Stenchikov G L *Soobshch. Prikl. Mat. VTs Akad. Nauk SSSR* (1985)
151. Aleksandrov V V, Stenchikov G L *Dokl. Akad. Nauk SSSR* **282** (6) 1324 (1985)
152. Stenchikov G L *Proc. Appl. Math. Comput. Center AS USSR* (1985)
153. Stenchikov G L, Carl P *Preprint AS GDR* (1985)
154. Stenchikov G L *Priroda* (6) 39 (1985)
155. Svirezhev Yu M *Priroda* (6) (1985)
156. Stenchikov G L, in *Klimaticheskie i Biologicheskie Posledstviya Atomnoĭ Voĭny* (Climatic and Biological Effect of Nuclear War) (Moscow, 1986) p. 66
157. Izrael' Yu A *Meteorologiya Gidrologiya* (10) 5 (1983)
158. Izrael' Yu A, Petrov V N, Severov D A *Meteorologiya Gidrologiya* (9) 5 (1983)
159. Izrael' Yu A *Dokl. Akad. Nauk SSSR* **281** (4) 821 (1985)
160. Izrael' Yu A, in *Klimaticheskie i Biologicheskie Posledstviya Atomnoĭ Voĭny* (Climatic and Biological Effect of Nuclear War) (Moscow, 1986) p. 46
161. Kondrat'ev K Ya, Baĭbakov S N, Nikol'skiĭ G A *Nauka v SSSR* (2) 2; (3) 3 (1985)
162. Turko R P et al. *Science* **222** 1282 (1983)
163. Covey C, Schneider S H, Thompson S L *Nature* (London) **308** 21 (1984)
164. Crutzen P J, Galbally L E, Brühl C *Clim. Change* **6** 323 (1984)
165. Schneider S H, in *Britannica Book* (1985) p. 27
166. Cattor W R *Am. Scientist* **73** 275 (1985)
167. *SCOPE 28 Environmental Consequences of Nuclear War* (Chichester: J Wiley & Sons, 1985) Vols 1, 2
168. Dotto L *Planet Earth in Jeopardy* (New York: J Wiley & Sons, 1986)
169. Alvarez E W et al. *Science* **208** (4448) 613 (1980)
170. Monin A S *Istoriya Zemli* (History of the Earth) (Leningrad: Nauka, 1977)